

# CHALMERS



## Percutaneous vs transcutaneous bone conduction hearing systems

- Cadaver head investigations and heat aspects

*Master of Science Thesis*

MAGNUS SMITH  
MARIA STEGBERG

Department of Signals and Systems  
*Division of Biomedical Engineering*  
CHALMERS UNIVERSITY OF TECHNOLOGY  
Göteborg, Sweden, 2007  
Report No. EX086/2007

## Abstract

A conventional “Percutaneous Bone Anchored Hearing Aid” (P-BAHA) is an important rehabilitation alternative for patients suffering from conductive or missed hearing loss. Even if such percutaneous implants have a reasonably low complication rate, there are some drawbacks reported.

A transcutaneous Bone Conduction Implant system (BCI) would have the main advantage that no percutaneous attachment is needed since the implanted transducer would be permanently embedded in the temporal bone. The audio processor signal would be transmitted through the intact skin using an induction loop system.

The aims of this thesis are to investigate temperature aspects of the BCI transducer due to input power and to compare the electro-acoustic performance of a P-BAHA to that of a BCI on a cadaver head.

The BCI transducer temperature rise as a result of input power was measured. From these measurements, thermal resistances were calculated and a temperature rise model was designed. The electro-acoustic performance was measured on a cadaver head with the P-BAHA placed in the parietal bone and the BCI placed 15 mm deep into the temporal bone. The vibration responses were then measured at both the ipsi- and the contralateral promontorium. The P-BAHA was a Baha<sup>®</sup> Classic 300 and the BCI consisted of a Vibrant<sup>®</sup> Soundbridge<sup>®</sup> with a Balanced Electromagnetic Separation Transducer (BEST<sup>™</sup>) attached to it.

It was found that the BCI has a low temperature rise at normal operating condition. It was also found that the ipsilateral output response was higher for the BCI than for the P-BAHA whereas the contralateral output response was poorer for the BCI than for the P-BAHA for main speech frequencies.

Based on the results in this thesis it is concluded that the BCI could be a realistic alternative to the P-BAHA and that temperature issues will not be a problem.

## **Acknowledgements**

We would like to thank our supervisor Professor Bo Håkansson for great help, support and ideas. We would also like to thank PhD students Roger Malmberg and Sabine Reinfeldt for helping us with equipment and MD Måns Eeg-Olofsson for his participation during the cadaver head measurements at Sahlgrenska University Hospital. Finally we thank our fellow students Per Östli and Alfred Andersson for encouraging us and sharing their work.

# Table of Contents

<b>1. Introduction</b>	<b>1</b>
<b>2. Theory</b>	<b>3</b>
2.1 Bone conduction	3
2.1.1 Major principles	3
2.1.2 Propagation of vibrations through the skull	3
2.2 Bone conduction transducers	3
2.2.1 BEST™	4
2.2.2 B71	5
2.2.3 Baha® Classic 300	5
2.3 MED-EL processor and inductive link	6
2.4 Heat tolerance in bone tissue	7
2.5 Thermal resistance	7
2.6 Sound Pressure Level (SPL)	8
2.7 Total harmonic distortion (THD)	8
<b>3. Methods and material</b>	<b>9</b>
3.1 Methods	9
3.1.1 Temperature investigations	9
3.1.1.1 Input impedance	9
3.1.1.2 Temperature measurements	10
3.1.1.3 Thermal resistance	13
3.1.1.4 Temperature at maximum input	14
3.1.2 Cadaver head investigations	15
3.1.2.1 Frequency response with constant electrical stimulation	16
3.1.2.2 Sound pressure output response	17
3.1.2.3 Total harmonic distortion	17
3.1.2.4 Input impedance	18
3.2 Apparatus	18
3.2.1 Artificial Mastoid	18
3.2.2 Agilent 35670A 4-Channel FFT Dynamic Signal Analyzer	18
3.2.3 Laser Doppler Vibrometer (LDV)	18
3.2.4 PULSE	18
<b>4. Results</b>	<b>20</b>
4.1 Temperature investigations	20
4.1.1 Input impedance of the transducers	20
4.1.2 Temperature development	23
4.1.3 Thermal resistance	25
4.1.4 Temperature model	28
4.1.5 Thermal resistance in skull bone	29
4.1.6 Temperature expectations using temperature model	31
4.1.7 Temperature at maximum input	34
4.2 Cadaver head investigations	36

4.2.1 Frequency response with constant electrical stimulation_____	36
4.2.2 Sound pressure output response and total harmonic distortion __	39
4.2.4 Input impedance of BAHA _____	43
<b>5. Discussion</b> _____	<b>44</b>
5.1 Thermal resistance _____	44
5.2 Output response _____	46
5.3 Frequency response_____	50
<b>6. Conclusion</b> _____	<b>53</b>
<b>References</b> _____	<b>54</b>
<b>Appendix A</b> _____	<b>55</b>
<b>Appendix B</b> _____	<b>57</b>

# 1. Introduction

It has been shown that implantable hearing devices, such as middle ear implants, can, in some cases, improve patient hearing ability in a better way than traditional external in-ear hearing aids. The same goes for bone conducting hearing aids. The bone anchored hearing aids used today are percutaneous, meaning that they are permanently perforating the skin. One disadvantage is that they require a certain amount of hygiene and care. However, they do not suffer from the disadvantages of the middle ear implants, for which the implant surgery is expensive and associated with risks of damage to the facial nerve.

Middle ear implants that connect to the middle ear bones are not used for patients with a diseased middle ear. Such patients can benefit from a bone conducting hearing aid to be able to hear. By combining the two techniques one could make use of the induction power transfer system in middle ear implants, and thereby shortening the time-to-market, and let the transducer be a bone anchored bone conduction type, completely embedded in the skull behind the ear. This possible design is illustrated in Figure 1. The surgical procedure would not be as crucial as the one mentioned above, mainly because the site of implantation would not be so close to the middle and inner ear, but rather a few centimetres deep in the temporal bone. Even though several studies of bone anchored hearing aids and their performance have been made, it is still not known exactly where to place an implanted bone conduction hearing aid to achieve the an optimal quality of sound.

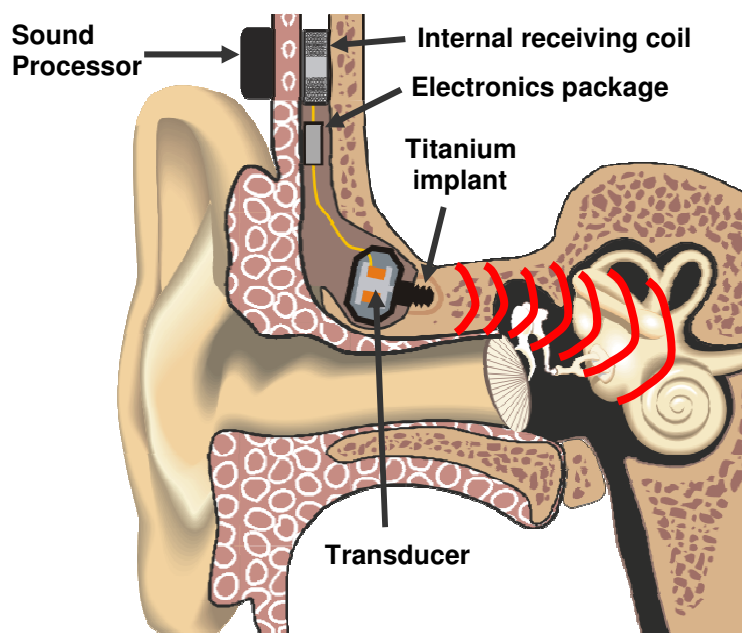


**Figure 1.** A transcutaneous bone conduction implant (BCI) with an implanted transducer, an external sound processor and a transcutaneous power transfer to the internal receiving coil [1].

This thesis is one step on the path towards realising the first implantable bone anchored hearing device. It covers two separate issues that need to be investigated before being able to make the product commercially available. We have combined the BEST<sup>TM</sup> transducer with the MED-EL Vibrant<sup>®</sup> Soundbridge<sup>®</sup> [2] to a transcutaneous bone conduction implant (BCI). From now on this combined device will be referred to as BCI.

The first part of the thesis aims to study the heat generation in the coil of the BEST<sup>TM</sup>. The temperature rise at normal operating conditions will then be deduced from this. The results will be compared to the heat tolerance of the skull bone, in order to establish whether or not the BEST<sup>TM</sup>, in its present form and with its present power demand, is suitable for implantation. It is also desirable to be able to model the temperature rise as a function of input power, in order to determine how much power the device can take before raising the temperature above a safe limit.

The second part of the thesis aims to investigate the output response as well as the distortion from the BCI-device implanted in the temporal bone/mastoid. These investigations will be performed on a cadaver head. The results will then be linked and compared to the results of another thesis project run parallel to this one. Comparisons to the commercially available percutaneous bone anchored hearing aid Baha<sup>®</sup> [3] will also be made. The main purpose of these studies is to further explore the possibilities of completely implanting a bone conduction hearing aid.

## **2. Theory**

### **2.1 Bone conduction**

The devices studied in this thesis are designed based on the principle of bone conducted hearing. It is therefore advisable to give some background on the nature of bone conduction.

#### **2.1.1 Major principles**

Bone conduction is a complex, yet natural phenomena. In short it means that vibrations in the skull, teeth and skin are transmitted through the skull bone to the cochlea and further on to the basilar membrane. Here the vibrations are coded by neurons and perceived as sound by the brain. Bone conduction makes up a part of our normal hearing experience [4]. Bone conduction devices are therefore good substitutes for people with hearing disabilities. Hearing aids based on bone conduction will help people who have mixed hearing loss, a damaged inner ear or conductive hearing loss. They might also help single sided deafness, since the sound vibrations can be transmitted from a device placed on the deaf side, to the functional cochlea on the other side.

#### **2.1.2 Propagation of vibrations through the skull**

For low frequencies the skull moves as a rigid body, giving response to vibrational stimulation mostly in the same direction as the stimulation itself [5]. However, at higher frequencies the skull inherits both resonances and antiresonances. The vibrations are propagated throughout the skull; hence sound can be transmitted from one side to the other. This consequently means that sound originating from one side can be transmitted through the skull to the cochlea on the other side.

Stenfelt concluded that vibrations in the skull were mainly transmitted via the bones of the cranial vault rather than through the base of the skull [5]. This would indicate that more superficial bone conduction stimulation results in a better stimulation of the contralateral cochlea. However a deeper placement of stimulus was found to give a better and more directional response at the ipsilateral cochlea, implying that an improved sensitivity to bone conducted sound can be obtained by implanting a bone-anchored device close to the cochlea [5].

### **2.2 Bone conduction transducers**

There are different transducers based on the bone conduction technique. This study however, focuses on the BEST<sup>TM</sup> (Balanced electromagnetic separation transducer), though both the B71 from Radioear Corp.(USA) and the Baha<sup>®</sup> Classic 300 transducers are used for means of comparison. Important features of such transducers are their input impedance, their resonance frequency, their distortion. Normally bone transducers are designed to have a resonance frequency close to the lowest frequency of interest. The input impedance determines what source is suitable to feed the transducer and consequently determines the power needed.



### 2.2.1 BEST™

The BEST™ (balanced electromagnetic separation transducer) is a relatively new bone conduction transducer developed at the Department of Signals and Systems, Chalmers University of Technology. The transducer has a linear magnetic flux versus force characteristic. This results in lower harmonic distortion compared to the traditional bone transducers [6]. This design also implies that the losses are minimized. Figure 2 shows the linear force versus magnetic flux and a cross sectional view of the BEST transducer.

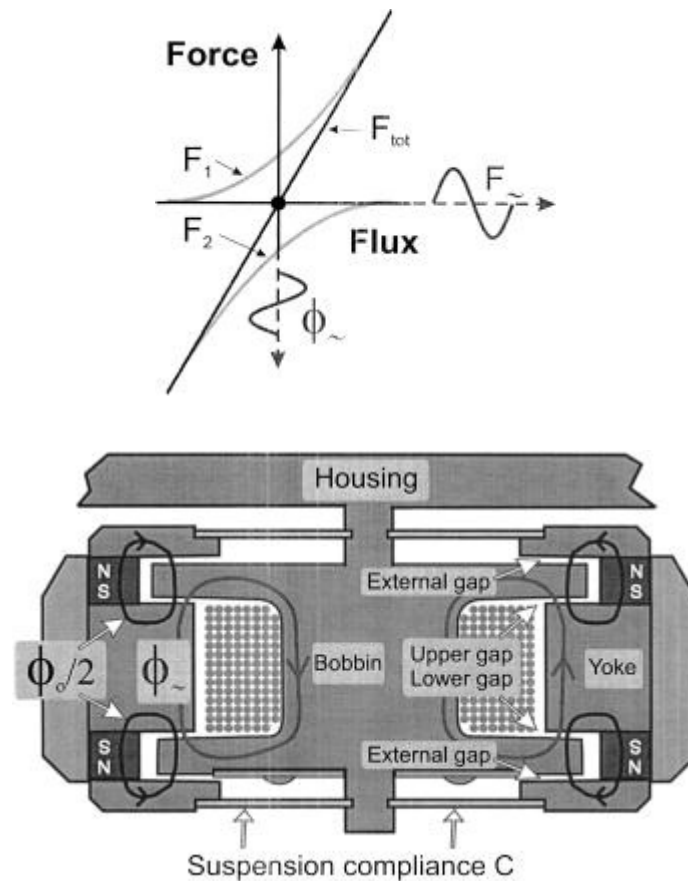


**Figure 2.** The force versus magnetic flux characteristics of the BEST™ and a cross-sectional view of the BEST™ [6].

The design also aims to balance or cancel out static forces within the construction. This principle allows a less stiff spring suspension and a lower free mass, yet still introduces lower distortion and a better low frequency response [6].

There are a few versions of the BEST transducer, where the main difference is the thickness of the coil wire. This gives the transducers different input impedances which in turn affects the power characteristics of the transducers. Studied in this thesis are BEST 90 and BEST 150, where 90 and 150 refers to the wire thickness and are of the magnitude  $\mu\text{m}$ . The coil wire in BEST 90 can tolerate more than  $100^{\circ}\text{C}$  but with some safe margin for other components in the design, the temperature should not be allowed to exceed  $80^{\circ}\text{C}$ .

### 2.2.2 B71

The B71 transducer is frequently used in hearing threshold testing and other audiology applications. The relation between magnetic flux and force is not linear but rather quadratic. Having a quadratic relation generates a higher level of primarily second harmonics, hence increasing the total distortion in the device. The specific device used for this study was encapsulated in a plastic housing. A cross sectional view of the B71 can be seen in Figure 3.

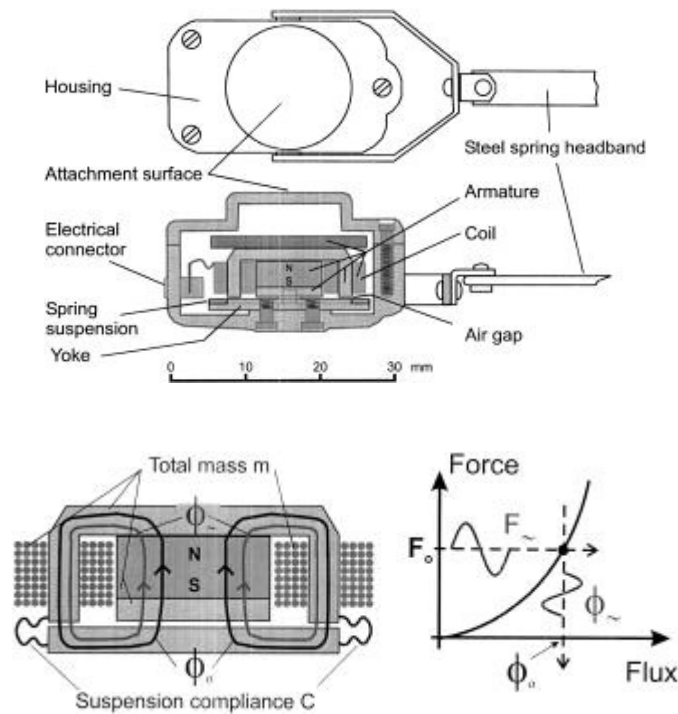


**Figure 3.** External view and cross-sectional sketch, close-up of the magnetic circuit of the B71 and a corresponding flux to force characteristic [6].

### 2.2.3 Baha<sup>®</sup> Classic 300

The Baha<sup>®</sup> Classic 300 transducer, from now on referred to as BAHA, is similar to the B71 transducer, though its spring suspension has inherent damping. It is part of a commercial bone-anchored hearing aid combining it with different sound processors. The one that has been used in this thesis is the Baha<sup>®</sup> Classic 300 processor. Figure 4 shows the Baha<sup>®</sup> Classic 300 and a sketch of the Baha<sup>®</sup> Classic 300 attached to the skull bone [3].

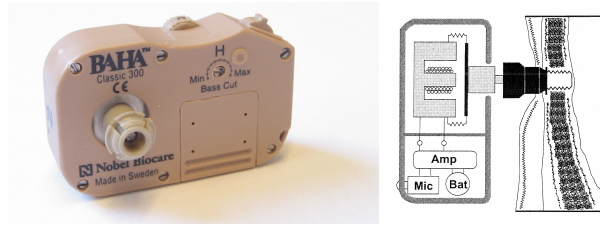


**Figure 4.** Picture of the Baha<sup>®</sup> Classic 300 and a sketch of it when it is percutaneously attached to an osseointegrated titanium implant.

### 2.3 MED-EL processor and inductive link

The MED-EL Vibrant<sup>®</sup> Soundbridge<sup>®</sup> is a middle ear implant that enhances vibrations of the ossicles via a floating mass transducer attached to the incus. Exterior is an audio processor that process sound into electrical signals. These are transcutaneously transmitted to the internal receiver of the Vibrant<sup>®</sup> Soundbridge<sup>®</sup>. The implanted unit then sends the signal via a conductor link to the floating mass attached to the incus, shown in Figure 5.

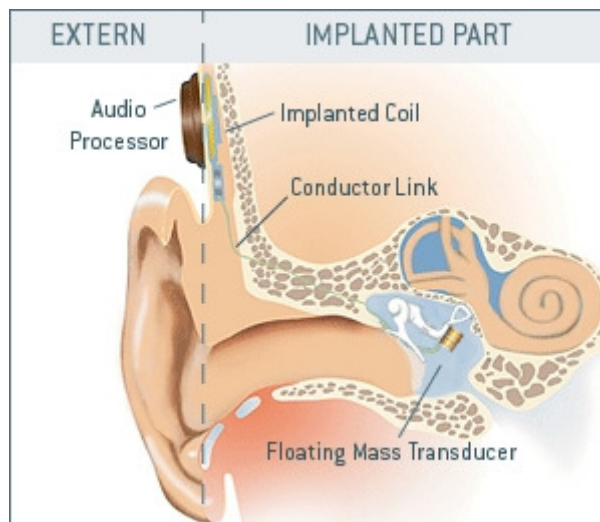


**Figure 5.** The MED-EL Vibrant<sup>®</sup> Soundbridge<sup>®</sup> [2].

The advantage with the Vibrant<sup>®</sup> Soundbridge<sup>®</sup> compared to air conduction hearing devices is that there are no parts in the ear canal that can irritate. Therefore the normal hearing is intact and only enhanced with the Vibrant<sup>®</sup> Soundbridge<sup>®</sup>. Compared to bone anchored hearing devices, it has a transcutaneous transfer thru the skin, held in place by a magnet. This reduces the risk of infections that percutaneous bone conduction devices struggle with [2].

One reason for using an implantable BEST transducer together with the audio processor, implanted coil and the conductor link of the Vibrant<sup>®</sup> Soundbridge<sup>®</sup> is that these are already certified for use inside the body. This would speed up the time for getting the whole system with the implanted BEST transducer out on the market.

## 2.4 Heat tolerance in bone tissue

Human tissue is sensitive to a relatively small rise in temperature. Remember that a fever of 40°C will make us rather ill. In bone there is a risk of necrosis at elevated temperatures. Studies have shown that a temperature as low as 42 - 45°C will cause damage to mammal bone tissue if the exposure time is long enough. Since mammals have approximately the same body temperature, this elevation in temperature is probably valid for humans too. It may also be pointed out that if the bone was exposed for 55°C for as little as 3 minutes; a widespread bone necrosis was detected [7].

Since heat will be generated by a foreign object inside the skull bone, it is important to know how well the bone will be able to lead away that heat. There are indications that the thermal conduction of bone tissue is rather low, hence making the bone acting as an insulator. What needs to be established then, is whether or not the bone at the implant site (mastoid) will be able to lead away enough heat for the local temperature to stay below a safety limit (40 - 42°C).

## 2.5 Thermal resistance

The concept of thermal resistance is widely known in semiconductor theory. The thermal resistance is a measure of the temperature rise due to power dissipation (°C/W). An equivalent circuit for the thermal resistance can be seen in Figure 6.

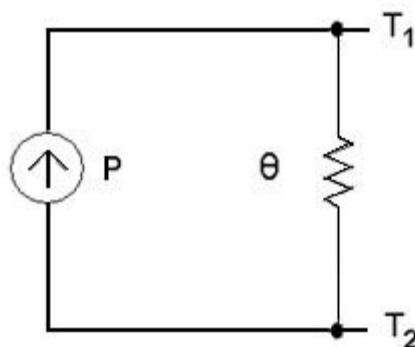


Figure 6. Thermal resistance equivalent circuit.

Given a certain maximum junction temperature and knowing the thermal resistance of a transistor, the amount of power that can be fed to the transistor without raising the junction temperature above its maximum can be deduced [8]. A similar theory could be useful in deciding what maximum power the BEST transducer can tolerate without having its coil temperature raised above a certain  $T_{max}$ . This is especially important if one wishes to implant the BEST transducer in the skull bone, as explained in the previous section.

## **2.6 Sound Pressure Level (SPL)**

The pressure of sound is often given in dB SPL, where SPL stands for sound pressure level. This is a relative value of the sound pressure and defined as decibel relative 20  $\mu$ Pa. This is approximately the threshold audibility level at 1 kHz for an average person [9].

## **2.7 Total harmonic distortion (THD)**

The total harmonic distortion at a frequency is the total power in the harmonics of that frequency divided by the power of the fundamental frequency.

$$THD = \frac{\sum f_1 \dots f_4}{f_0} \cdot 100\%$$

The THD is given in percent of the fundamental energy. Resonance peaks further up in the spectra might therefore result in high distortion at lower frequencies. The THD will give a measure of the linearity of an amplifier [10].

## 3. Methods and material

### 3.1 Methods

This section is divided in two parts since the scope of the thesis has two focuses. The first part covers the methods used for investigating the thermal resistance and the temperature behaviour of the BEST transducer. Thereafter the second part, which describes the methods used for measuring frequency and output responses along with total harmonic distortions for the BEST and the BAHA transducers, will follow.

#### 3.1.1 Temperature investigations

For the temperature investigations, three different devices were used; a BEST 90 transducer, a BEST 150 transducer and a B71 transducer, all encapsulated in their housings. To begin with, the input impedance of all transducers was measured, since it affects the power to the transducers. Thereafter the temperature rise in the transducer due to input power was measured and the thermal resistance calculated. Finally, a measurement of the temperature at a certain fixed maximum input was done. All methods are described in the following sections.

##### 3.1.1.1 Input impedance

For each transducer, the input impedance for all frequencies between 100 Hz -10 kHz was measured using the Agilent 35670A dynamic signal analyzer. For BEST 90, the impedance was measured without housing and with the transducer attached to a skull simulator, TU 1000. For the other two transducers, BEST 150 and B71, the impedance was measured when the transducer was inside its housing and placed in the fixture later used for the temperature measurements (Figure 7). This was to guarantee that the impedance was correct with respect to the settings at which the temperature would later be measured.

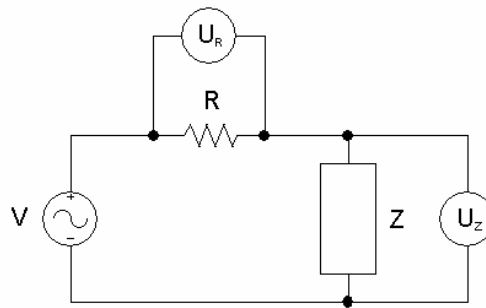


Figure 7. The temperature measurement setup.

The impedance was then used to calculate the active power applied to the transducer at a specific frequency. In the input impedance measurements, a resistance of  $100\ \Omega$  was connected in series with the transducer. A swept sine of frequencies between  $100\ \text{Hz}$  -  $10\ \text{kHz}$  with the amplitude of  $0.5V_{\text{rms}}$  was applied to the circuit and the voltage across the resistance and the transducer was measured respectively. A schematic of the circuit is shown in Figure 8. The impedance was calculated as follows:

$$i = \frac{U_R}{R}$$

$$Z = \frac{U_Z}{i}$$



**Figure 8.** Circuit used to measure the input impedance,  $Z$ , of each transducer.

### 3.1.1.2 Temperature measurements

The temperature generated by the transducer was measured using two Pt-Ni thermocouples; one attached to the transducer coil and one attached to the external fixture (the screw attaching the transducer to its housing), using a thermally conductive silicon paste (ACC Silicones). The transducer housing was cut open in order to allow placement of the coil thermocouple. To ensure that the thermocouples were held in place throughout the measurements, the transducer was placed in a purpose built fixture (Figure 7). Both thermocouples were connected to INOR MinIPAQ-L intelligent 2-wire transmitters. The transmitters were connected via two  $270\ \Omega$  resistors to an NI USB-6009 data acquisitioner. The transducer was fed with DC voltages via an Oltronix power supply (C15-2D) and AC voltages via a frequency generator (Wavetek 5MHz Sweep Generator, model 184) followed by a power amplifier (Brüel & Kjaer, type 2706). The power amplifier was needed since the output impedance of the frequency generator is far greater than the input impedance of the transducer,  $50\ \Omega$  compared to  $14.7\ \Omega$  and  $3.4\ \Omega$ . An illustration of the temperature measurement setup can be seen in Figure 9.

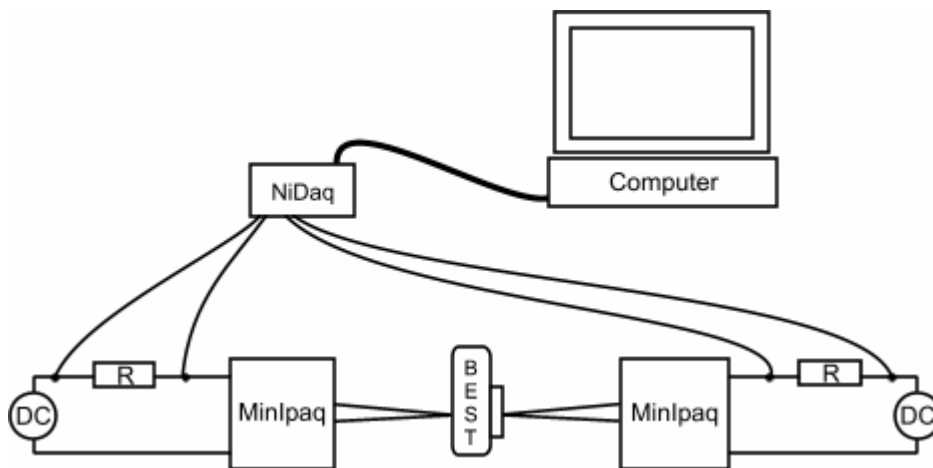


**Figure 9.** Setup for measuring the temperature generated by the transducers.

The transducer coil is fixed to the housing via a bobbin core and a screw fixture. Around the coil there is a free mass, the vibration element, only connected to the bobbin and housing via a spring suspension. The heat developed in the coil can mainly be lead away through the screw fixture, which is small and has poor thermal conductivity. Heat will not significantly be passed on to the free mass, because of the equally poor thermal conductivity of air and the small connection to the coil, the spring suspension and the screw fixture. Therefore, most of the heat dissipated in the coil will remain there. This is undesirable, since too much heat will damage the materials and be harmful if implanted. One solution to this problem may be to increase heat transfer between the coil inside the housing and the outside air (ambient). This will be tested by inserting a thermally conductive paste into the screw fixture. The same measurements as for the original BEST will be repeated for the BEST with thermally conductive paste.

Temperature measurements were done at both DC and AC voltages. To begin with, a measurements at room temperature was recorded, and then the voltage was applied to the circuit, while still recording data from the thermocouples. Each test sequence was run for at least 20 minutes to account for the temperature rise time. After finishing the first series of measurements, thermally conductive paste was inserted under the fixture of both BESTs in order to increase the thermal conduction between the coil and the external fixture. A summary of what frequencies and what voltages were used for each test series can be found in Tables 1-3.



## BEST 90

Unaltered		Thermally conductive paste	
<i>Frequency [Hz]</i>	<i>Input Voltages [V<sub>rms</sub>]</i>	<i>Frequency [Hz]</i>	<i>Input Voltages [V<sub>rms</sub>]</i>
0 (DC)	1 / 1.5 / 2	0 (DC)	1 / 1.5 / 1.7 / 2
100	1.5 / 1.6	100	1.5 / 2
200	1.8 / 2 / 2.1	200	1.5 / 2
400	1 / 2 / 2.5	300	1.5 / 2
4000	1 / 2	400	1.6 / 2 / 2.1

**Table 1.** Specification of the signal applied to the BEST 90 transducer.

Preliminary tests showed that the amplitude could not be as high for BEST 150 as for BEST 90, simply because they have different input impedances.

## BEST 150

Unaltered		Thermally conductive paste	
<i>Frequency [Hz]</i>	<i>Input Voltages [V<sub>rms</sub>]</i>	<i>Frequency [Hz]</i>	<i>Input Voltages [V<sub>rms</sub>]</i>
0 (DC)	0.6 / 0.7 / 0.8 / 1	0 (DC)	1
100	0.7 / 0.8 / 1	100	1
150	0.7 / 0.8	200	0.8
200	0.7 / 0.8	300	0.8
250	0.7 / 0.8	400	0.8
300	0.7 / 0.8	500	0.6
350	0.7 / 0.8	1000	1.8
400	0.65 / 0.7 / 0.8	1500	1.8
500	0.6	2000	2.4
600	0.6	2500	2.4
700	0.6 / 1	3000	2.8
800	0.7 / 1	3500	3.4
900	0.7 / 0.8 / 1.5	4000	3.4
1000	1 / 1.1 / 1.8		
1500	1.5		
2000	2.4		
3000	2 / 2.8		
4000	3.4 / 3.5		

**Table 2.** Specification of the signal applied to the BEST 150 transducer.

For the B71 transducer it was decided to exclude 3 kHz from the measurement series, since there is a resonance at that frequency, meaning that less power can be applied, hence the heat generation will be considerably lower.

### B 71

Unaltered	
<i>Frequency [Hz]</i>	<i>Input Voltages [V<sub>rms</sub>]</i>
0 (DC)	1
100	1
200	0.8
300	0.8
400	0.8
500	0.5
800	0.8
900	0.8
1000	1.8
1500	1.8
2000	3
2500	3
4000	3

**Table 3.** Specification of the signal applied to the B71 transducer.

In order to obtain some reference as to what the thermal resistance of bone tissue might be; heat transfer measurements were also done on a dry piece of parietal bone. A 270  $\Omega$  resistance was, together with one of the thermocouples, attached to the outside of the bone using the thermally conductive paste. The other thermocouple was attached in the same manner to the other side of the bone specimen. Given this setup, the temperature developed in the resistance attached to the outside of the bone and the temperature on the opposite side of the bone could be measured, assuming that this could give some indication on the thermal resistance of skull bone.

#### 3.1.1.3 Thermal resistance

Figure 10 shows the basic electrical equivalent of the thermal process inside the transducer.  $P$  is the heat power developed in the copper coil, due to the resistance of the copper wire.  $\theta_{cf}$  is the thermal resistance between the coil and the external fixture.  $\theta_{fa}$  is the thermal resistance between the external fixture and the ambient.

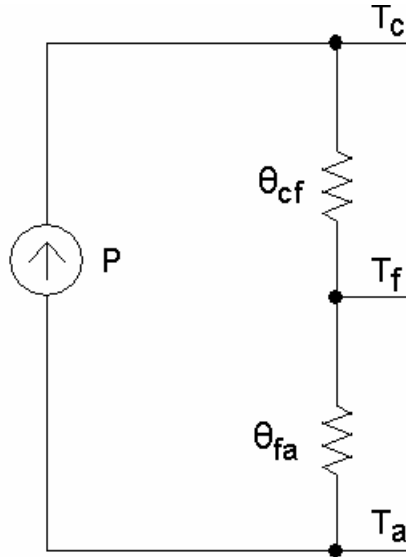


**Figure 10.** Equivalent electrical circuit of the thermal process.  $T_a$ ,  $T_f$  and  $T_c$  are the ambient temperature, fixture temperature and coil temperature respectively.

After measuring the temperature of the coil ( $T_c$ ) and the fixture ( $T_f$ ) at different input voltages and frequencies, the corresponding thermal resistances,  $\theta_{cf}$  and  $\theta_{fa}$  were determined. They were calculated according to the following equations:

$$\theta_{cf} = \frac{(T_c - T_f)}{P},$$

and

$$\theta_{fa} = \frac{(T_f - T_a)}{P},$$

where the ambient temperature ( $T_a$ ) was assumed to be constant and was measured with an analogue thermometer. The thermal resistances were then to be used to calculate a maximum input voltage for each BEST transducer, given maximum values for  $T_c$  or  $T_f$ .

Knowing the maximum output of the Vibrant<sup>®</sup> Soundbridge<sup>®</sup>, one can also calculate the temperature rise in the coil of the BEST transducer, when it is driven by the Vibrant<sup>®</sup> Soundbridge<sup>®</sup>.

Based on the thermal resistances, calculations describing what maximum input voltage will be allowed before the coil temperature is increased by five degrees Celsius, were also done. The idea of this step was to see what input voltages were needed to increase the transducer temperature to a level equal to the maximum temperature that the body tissue can withstand.

#### 3.1.1.4 Temperature at maximum input

It is also of interest to find out what coil and fixture temperature is reached when overloading the BEST. But first, in order for this paragraph to make

sense, one needs to define what the maximum input is. Previous tests have been conducted at input levels that give an output THD of 5.5 % or an output voltage of  $4V_{\text{rms}}$ , measured using the Artificial Mastoid type 4930 (Brüel & Kjaer) [9]. During some of these tests, the BEST 90 transducer was destroyed, which is why it might be of interest to know what temperatures are reached near the destruction point. Measuring at maximum input will also give an opportunity to verify the temperature rise model.

Three BEST transducers encapsulated in housings were used. One thermocouple was fixed onto the external fixture using the thermally conductive paste, as in 3.1.1.2. The thermocouple was also secured using a piece of medical tape. The BEST was then placed in the artificial mastoid. The Agilent 35670A dynamic signal analyzer was used as a signal source, setting it to a fixed sine at specific frequencies presented in the results. The artificial mastoid output was also connected to the Agilent for FFT-analysis, power spectra measurements. By letting the Agilent find the first harmonic component in the spectra and then calculate the THD at that input frequency, the maximum input requirement could be determined.

### 3.1.2 Cadaver head investigations

For the second part of this thesis the electro-acoustic performance of an implantable bone conduction device was to be evaluated. Free field output response, total harmonic distortion and frequency response at constant electrical stimulation were the performance factors that were investigated.

All measurements were performed on a human cadaver head. The bone conduction devices being tested were attached to the skull in two different positions, one percutaneous and one transcutaneous. Position A was the conventional transcutaneous BAHA position, approximately 55 mm backwards and slightly upwards in the parietal bone. Position B was located approximately 14 mm deep into the temporal bone, following a mastoid ectomy. The two positions are illustrated in Figure 11.

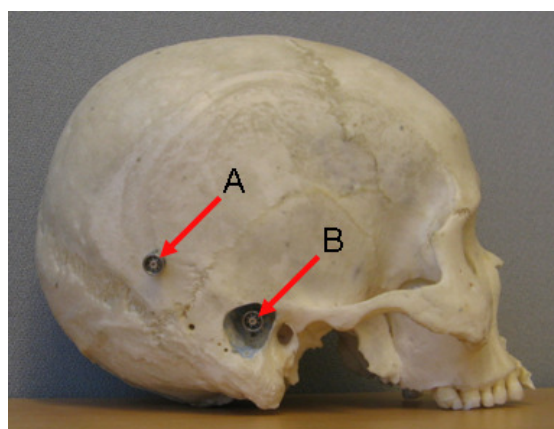


**Figure 11.** Positions of the transducer abutments.

For both the electrical response and the sound pressure response the vibration of the skull, the output velocity, was measured using a Laser Doppler Vibrometer (LDV). The sensitivity was set to 1mm/s/V, the low pass filter with cut-off frequency 15 kHz and the high pass filter set to 'on'. Tiny reflectors (weave type reflective material from common snap-on reflectors by 3M 'scotchlite') were glued on to the bones in both the right and the left inner ear, at the promontorium. The glue that was used was a gel-based glue (Loctite 454). The laser beam was pointed at the reflectors, so that the vibrations in the bone were reflected back to the LDV, which then registered the movement. Output velocity was measured both at the ipsilateral and contralateral side for stimulation at the subjects right parietal bone/mastoid. The skull bone vibrates in all directions, however, the direction of the vibrations measured by the LDV was, in this study, horizontally directed straight in from the ear canal opening, pointing medially towards the midplane of the skull. An illustration of the measurement setup can be found in Figure 12.

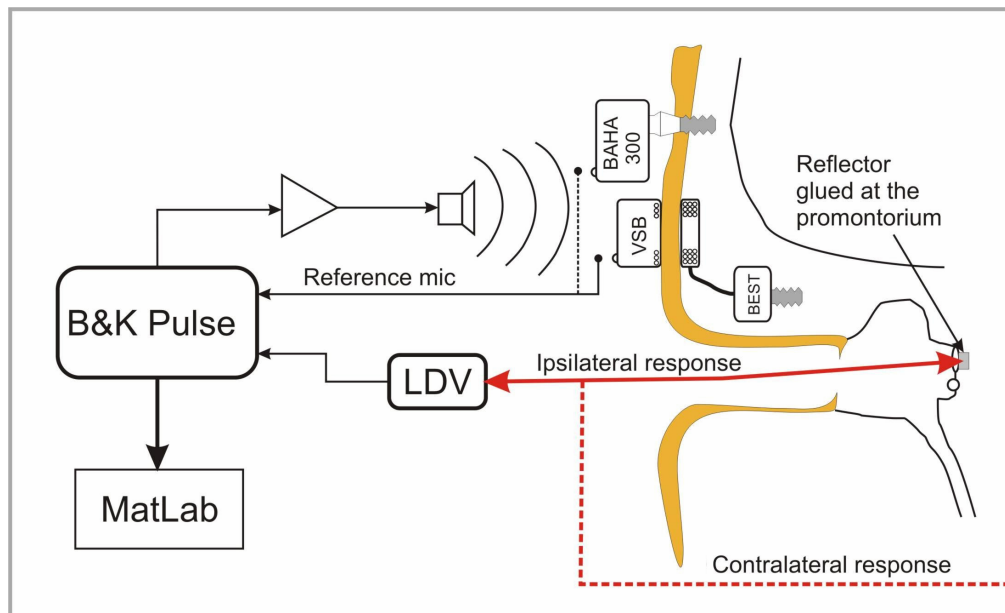


**Figure 12.** Measurement setup for the cadaver head investigations [1].

### 3.1.2.1 Frequency response with constant electrical stimulation

For the electrical response, the free transducers (BEST 90 transducer and the BAHA transducer) were connected to the implanted fixture via a snap coupling. The source of excitation was PULSE software and front-end (Brüel & Kjaer), generating a voltage of 50 mV at frequencies in the range of 100 Hz - 10 kHz with a resolution of 1/24 octave. The output signal from PULSE was amplified 20 dB to 0.5 V with an amplifier (Rotel RB-976MkII). The output from the amplifier was then directly connected to the transducers. For both transducers, the electrical response, in terms of vibration velocity of the bones in the inner ear, was measured ipsi- and contralaterally for both position A and position B.

### 3.1.2.2 Sound pressure output response

The sound pressure response was measured at constant sound pressure levels (SPL), 60 dB, 70 dB and 90 dB. Since the room characteristics were complex the sound pressure at the processor microphone needed to be corrected in order to achieve a constant level. This was done by making a first measurement of the SPL at the processor microphone using a reference microphone (Brüel & Kjaer condenser microphone type 4134). PULSE used the reference SPL curve to calculate an equalisation function used to correctly scale the output voltage, in order to compensate for the room dynamics and provide a constant SPL at the processor microphone.

The measurement setup was more or less the same as for the electrical response measurements, however instead of connecting the amplifier output to the transducer directly; it was connected to a speaker (HECO Odeon 100). The speaker was placed hanging from a stand in close proximity to the processor and reference microphone. Once the speaker output was equalised, real measurements could be done.

The BEST transducer device was connected to the MED-EL processor via the inductive link to form a transcutaneous bone conduction implant (BCI). As mentioned in the introduction this device is referred to as BCI. The output response resulting from the BCI was measured at both the ipsilateral and the contralateral promontorium with the BEST attached to both position A and position B. Two BAHA devices were also used for measuring the output response. As was the case for the BCI, the output response was measured at the ipsilateral and the contralateral promontorium, however the BAHA devices were only attached to position A. For the tests with the BAHA, the Classic 300 processor was used. The processor settings for each device can be seen in Table 4.

Device	Processor	Settings
BCI	MED-EL	Factory settings
BAHA 1	Classic 300	VC = 2, tone switch = N, BASS Cut = max
BAHA 2	Classic 300	VC = 2, tone switch = N, BASS Cut = max

**Table 4.** Settings for the processors used for the sound pressure output response and distortion measurements.

### 3.1.2.3 Total harmonic distortion

The total harmonic distortion (THD) at both the ipsi- and the contralateral side was also measured with the BCI in both positions (A and B) and with the two BAHA devices in position A. For the THD measurements the same setup as in 3.1.2.2 (sound pressure output response) was used. The THD measurements were performed at 70 dB SPL ranging in frequency from 100 Hz - 10 kHz. PULSE allows the user to choose how many harmonics will be used for calculating the THD. Only the first five harmonics were used since harmonics higher up in the spectra are not likely to be within hearing range.

#### **3.1.2.4 Input impedance**

Knowing the input impedance of the transducer is useful when analyzing the response and THD results. Since the input impedance of BEST 90 was already measured as described in section 3.1.1.1, it will not be described here.

Therefore only the input impedance of the BAHA needed to be measured. The procedure was more or less the same, though instead of a 100  $\Omega$  resistance, a 10  $\Omega$  was used.

### **3.2 Apparatus**

A variety of equipment was used during this study. Some of the equipment are more important and will therefore be further described in this section.

#### **3.2.1 Artificial Mastoid**

The artificial mastoid type 4930 incorporates a mechanical coupler or simulator of the human head and a force transducer. The force transducer measures the output of the device attached to the mastoid. This equipment is used to measure the frequency response and output of bone vibrators. It simulates the real-life situation where a vibrator is placed on the mastoid. It can be very useful when evaluating the performance of a new bone transducer, since it is more readily available than cadavers, which would otherwise be the preferred subject [12].

#### **3.2.2 Agilent 35670A 4-Channel FFT Dynamic Signal Analyzer**

The Agilent can be used for many different applications of signal analysis. It can not only receive signals but can function as a signal source as well. The Agilent is used either with swept sine or with FFT analysis. The swept sine function has been used to measure input impedances meanwhile FFT analysis mode was used when calculating the THD. One disadvantage with the THD calculation is that it can only measure the THD at one frequency at a time. Therefore this function was used only for measuring THD at a few frequencies [13].

#### **3.2.3 Laser Doppler Vibrometer (LDV)**

To measure the output frequency responses, an LDV (Polytec HLV-1000), specifically designed to be used in hearing studies, was used. The LDV sends out a laser beam pointed towards the point at which the velocity will be measured. At that point some kind of reflector must be positioned, in order to reflect the laser back to the LDV. The Doppler Effect is used to determine the velocity of the measurement point. As it is, the LDV only measures vibrations in one direction; tangentially to the laser beam [14].

#### **3.2.4 PULSE**

PULSE is a platform for noise and vibration analysis by Brüel & Kjaer. It was used for the cadaver head measurements to obtain the output response, frequency response and THD. It has several input channels, making it possible to measure several different properties at once, for example THD and frequency response. PULSE also facilitates complex user defined

measurement tasks. The platform is connected to a normal PC on which all the analyses are performed in the PULSE LabShop 11.1. The platform can also be used as a signal generator.

The Pulse system can derive the THD by sweeping through the range of frequencies. This clearly simplifies the THD measurements compared to using the Agilent signal analyzer, which can only handle FFT-analysis of one frequency and its harmonics in one measurement and therefore only gives one THD component in the frequency range.

The specific equipment used was the portable data acquisition unit 3560c, and PULSE LabShop 11.1 installed on a laptop PC. There is a special feature called Bridge to MATLAB<sup>®</sup>, which allows the user to transfer measurement data from PULSE to MATLAB<sup>®</sup> for post-processing and graphic display.

Other unique features are that the required measurement accuracy can be chosen prior to the measurement and that the Pulse system allows equalization of an output signal. By measuring the output response at the microphone using a swept sine with constant amplitude as the output signal, one can compensate a rise at a certain frequency of the output response by using the inverse output response as output signal next time. This means that post-processing tasks such as corrections are not needed and a constant level of sound pressure can be delivered to the microphone of the device under test [12].



## 4. Results

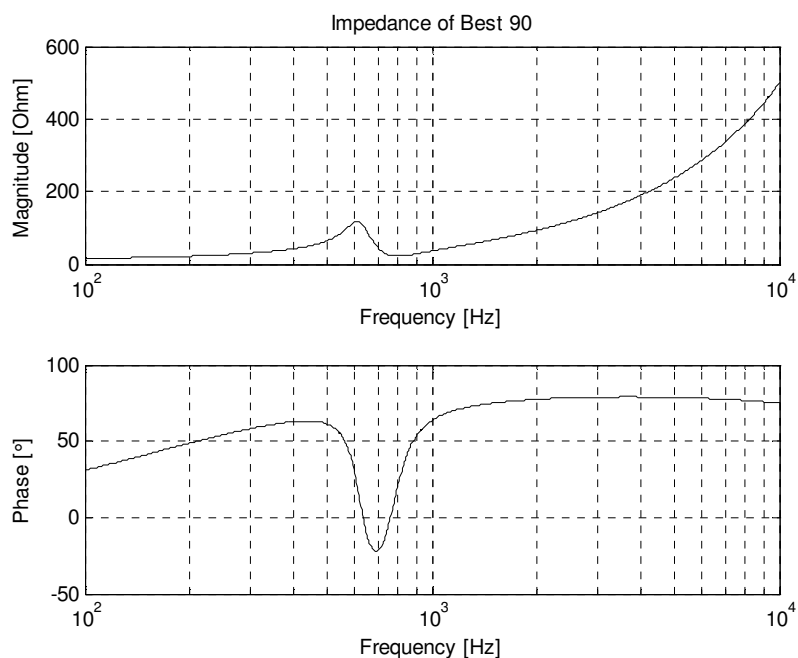
The results section is divided into two parts, where the first part concerns the temperature investigations and the second part concerns the cadaver head investigations of frequency and output response, along with the total harmonic distortion.

### 4.1 Temperature investigations

#### 4.1.1 Input impedance of the transducers

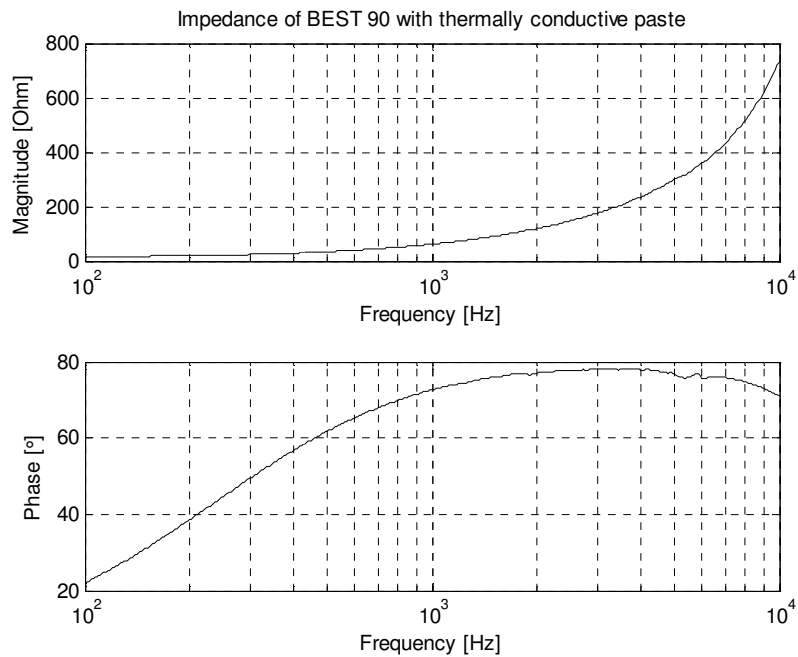
The input impedance for each transducer used in the thermal measurements is presented below in Figures 13-17.

Figure 13 shows the input impedance of BEST 90 without thermally conductive paste.



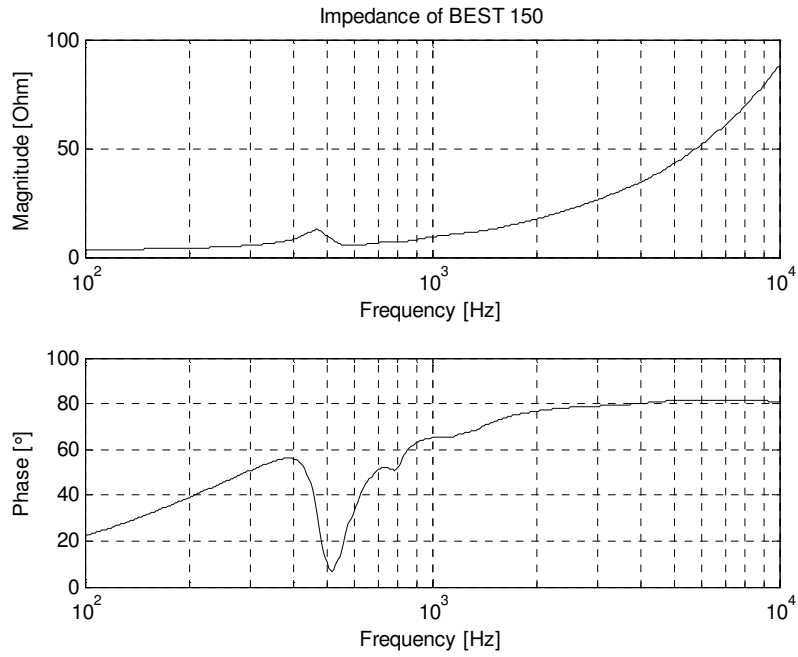
**Figure 13.** Input impedance magnitude and phase of BEST 90 transducer connected to the skull simulator.

Figure 14 shows the input impedance of BEST 90 with the thermally conductive paste.



**Figure 14.** Input impedance magnitude and phase of BEST 90 with thermally conductive paste, measured when the transducer was cased in its housing and placed in the temperature measurements fixture.

It must be pointed out that the resonance was completely attenuated when the thermally conductive paste was inserted in the BEST 90. By mistake the paste connected the coil to the free mass, which consequently no longer was free. However, since the temperature rise is due to the coil resistance, there is no reason to believe that this will affect the subsequent results for the thermal resistance  $\theta$ , since  $\theta$  should be material dependent and not frequency dependent.



**Figure 15.** Input impedance magnitude and phase of BEST 150. Measured in housing and temperature fixture.

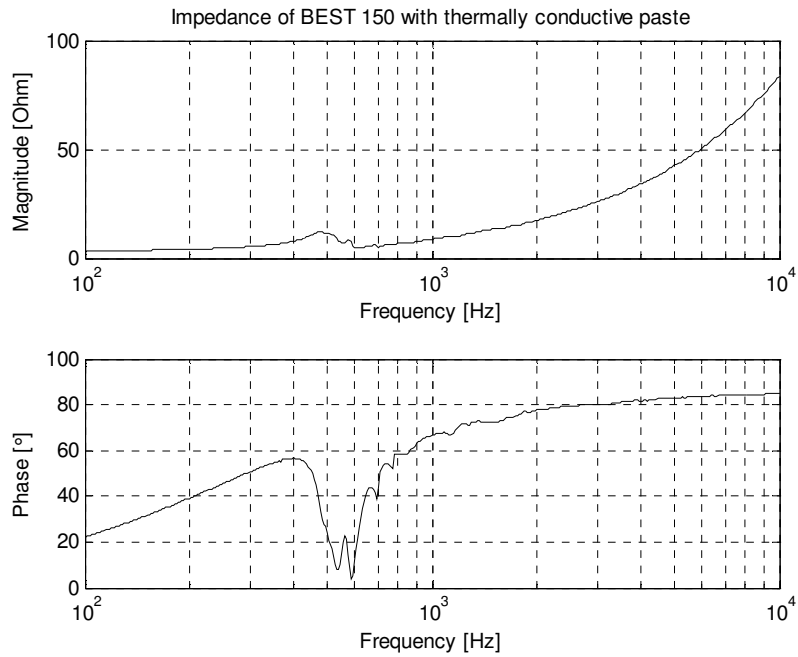


**Figure 16.** Input impedance magnitude and phase of BEST 150 with thermally conductive paste. Measured in housing and temperature fixture.

The phase shift is altered after inserting the thermally conductive paste, though according to previous assumptions (material specific not frequency dependant) this will not affect the results for  $\theta$ . The impedance of BEST 150 is significantly lower than that of BEST 90. This will be of importance for the input power calculations and therefore also for the calculations of  $\theta$ .

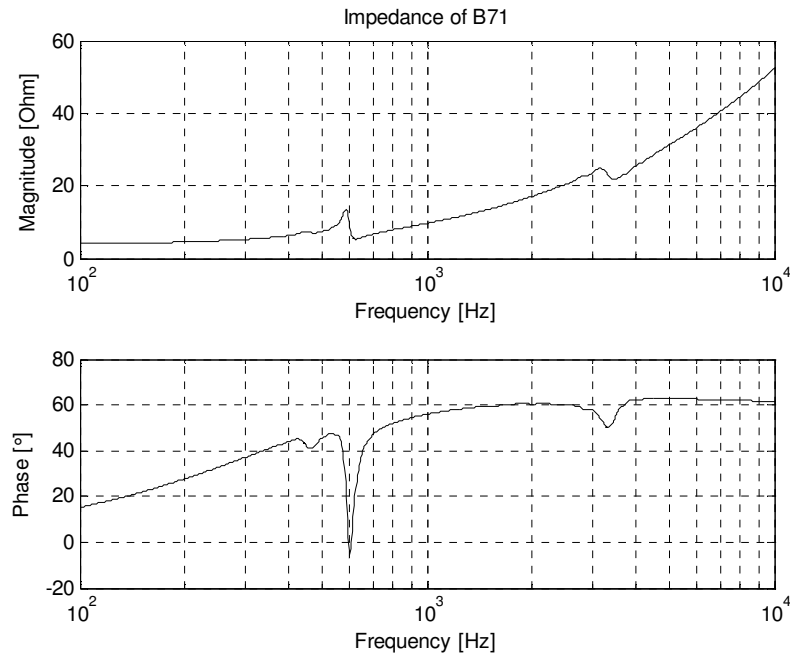


**Figure 17.** Input impedance magnitude and phase of B71. Measured in housing and temperature fixture.

#### 4.1.2 Temperature development

Two of the temperature measurements are plotted in this section to give the reader an idea of what the temperature rise might look like (see Figure 18 and Figure 19). The first measurement is for BEST 90 at 100 Hz and the other one is for B71 at 100 Hz. Both of these plots are good representatives of the temperature rise in each transducer. There is no plot for BEST 150 since its temperature rise curve is more or less identical to the curve for BEST 90, except for the final temperature to which it rises. The reason for this is that the two transducers have different input impedances and therefore the input power will be different although the input voltage is the same.

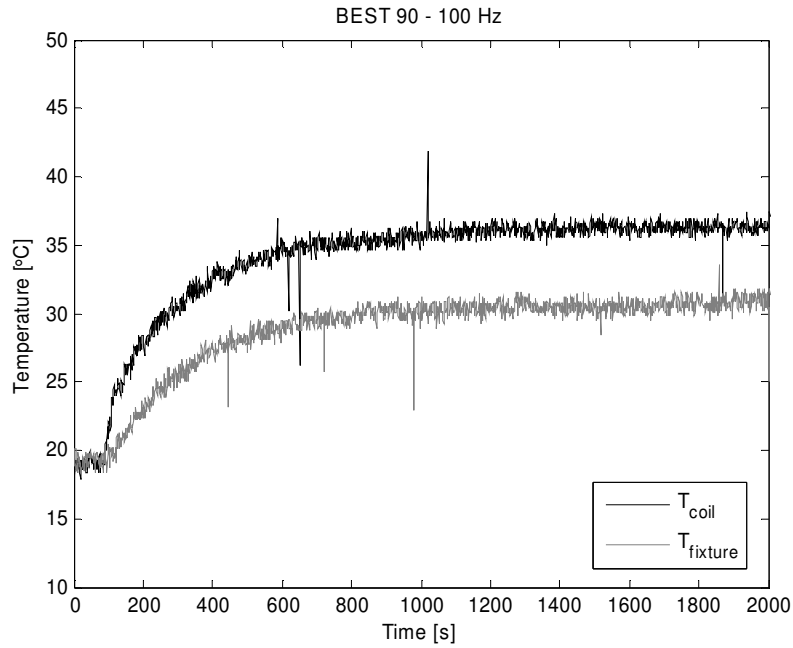


**Figure 18.** Temperature measurement of BEST 90 without paste.  $F = 100$  Hz,  $U = 1.5 V_{\text{rms}}$ , corresponds to 120 mW.

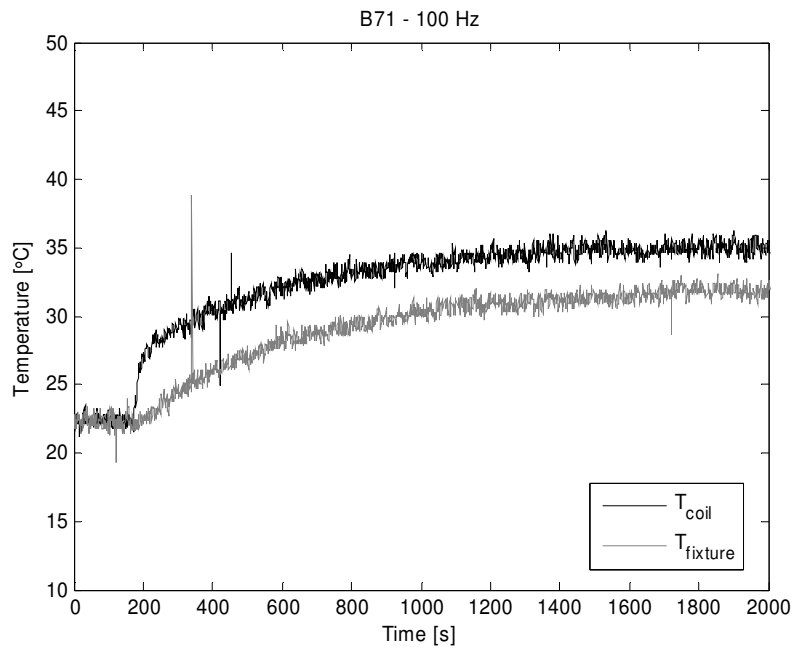


**Figure 19.** Temperature measurement of B71.  $F = 100$  Hz,  $U = 1 V_{\text{rms}}$ , corresponds to 240 mW.

Figures 18 and 19 show a difference in rise time between BEST and B71. The rise time for the BEST 90 transducer is approximately 10 minutes whereas the B71 rise time is approximately 15 minutes.

The temperatures reached during each measurement are presented in the Tables in Appendix A.

### 4.1.3 Thermal resistance

There is no reason to believe that the thermal resistance will vary with the frequency, since, as was stated in 4.1.1, the temperature rise is mainly due to the frequency independent coil resistance. After several measurements on each transducer with different frequencies the thermal resistance could be evaluated. In Figure 20 below the thermal resistance for the BEST 90 is shown.

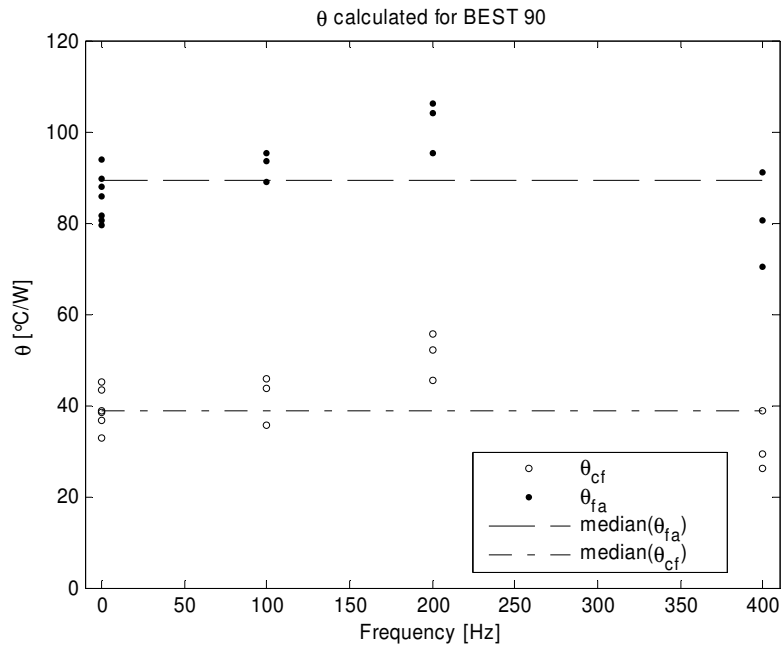


**Figure 20.** The thermal resistances for different frequencies in BEST 90. The median values for  $\theta_{fa}$  and  $\theta_{cf}$  are 90°C/W and 40°C/W respectively.

When thermally conductive paste was applied between the bobbin and the fixture, the calculated thermal resistance values changed as seen in Figure 21 below.

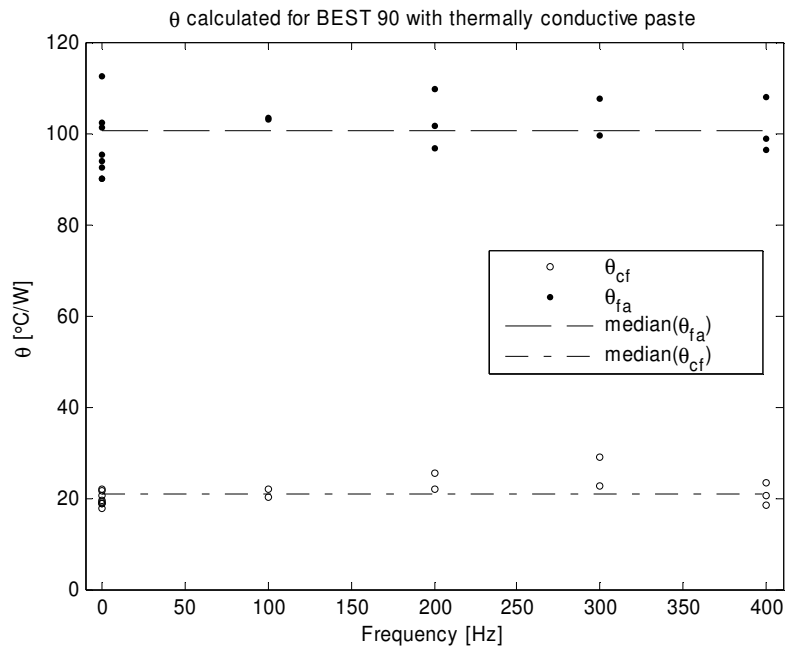


**Figure 21.** The thermal resistances for different frequencies in BEST 90 with thermally conductive paste. The median values for  $\theta_{fa}$  and  $\theta_{cf}$  are  $100^{\circ}\text{C}/\text{W}$  and  $20^{\circ}\text{C}/\text{W}$  respectively.

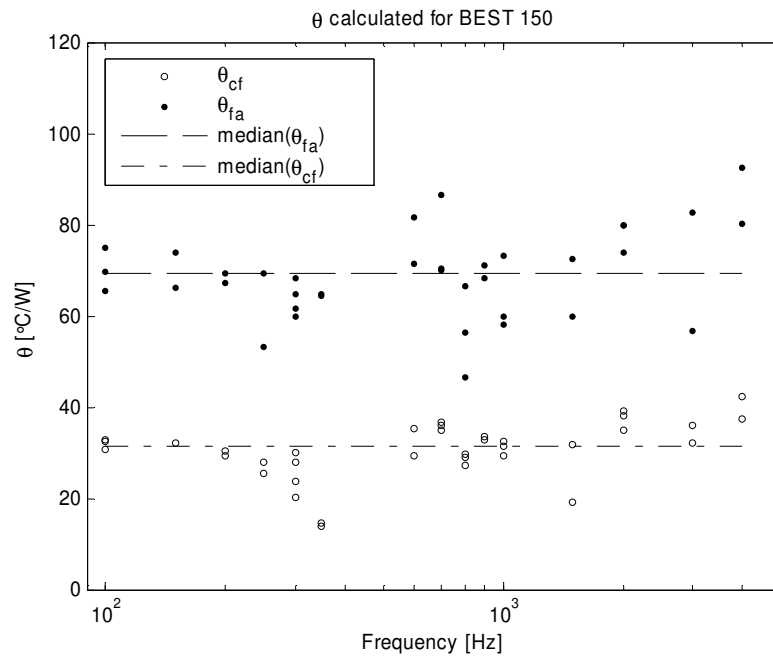


**Figure 22.** The thermal resistances for different frequencies in BEST 150. The median values for  $\theta_{fa}$  and  $\theta_{cf}$  are  $70^{\circ}\text{C}/\text{W}$  and  $30^{\circ}\text{C}/\text{W}$  respectively.

Looking at Figure 22, it will be noted that there are no  $\theta$ -values for 500 Hz. These were not plotted since they were negative and therefore inconclusive. The reason for this is that both the coil and the fixture temperature were almost identical.

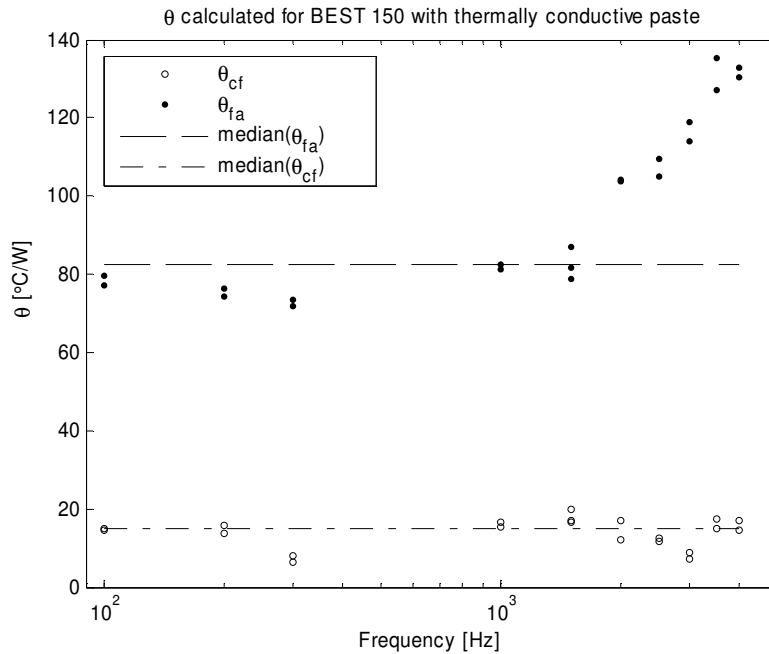


**Figure 23.** The thermal resistances for different frequencies in BEST 150 with thermally conductive paste. The median values for  $\theta_{fa}$  and  $\theta_{cf}$  are  $80^{\circ}\text{C}/\text{W}$  and  $17^{\circ}\text{C}/\text{W}$  respectively.

There is a remarkable rise for  $\theta_{fa}$  after 1.5 kHz that has not been seen in any of the other measurements. One can only speculate in why this phenomenon occurs, however no real explanation was found.



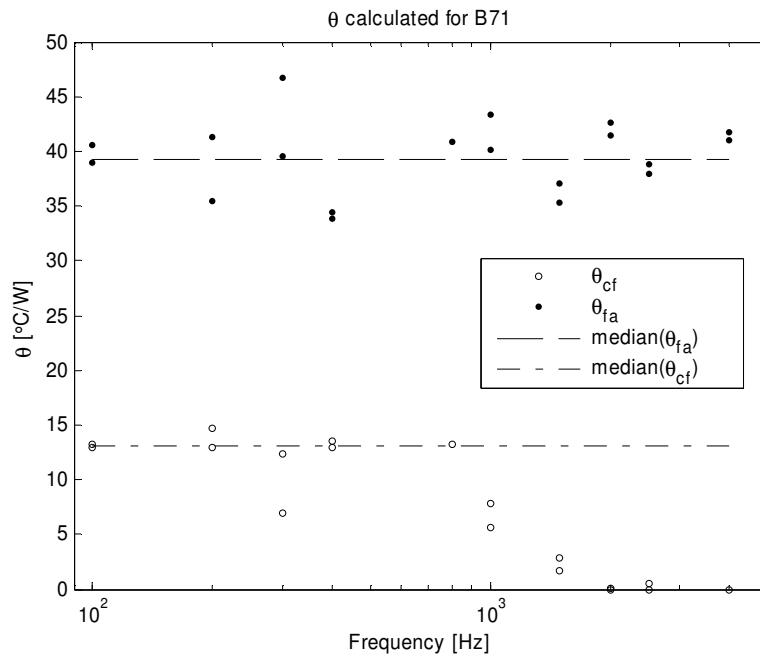


**Figure 24.** The thermal resistances for different frequencies in B71. The median values for  $\theta_{fa}$  and  $\theta_{cf}$  are approximately  $40^{\circ}\text{C}/\text{W}$  and  $15^{\circ}\text{C}/\text{W}$  respectively.

For frequencies above 1 kHz,  $\theta_{cf}$  unexpectedly decreases. One can speculate that this phenomenon is due to magnetic eddy currents in the bobbin that give extra heat generation to the transducer.

#### 4.1.4 Temperature model

The temperature rise has a start-up time transient, and will, consequently, not be instantaneous. Therefore, in order to properly model the temperature development in the transducer, the equivalent circuit of the thermal conduction process (Figure 10) needed to be modified to fit the time transient. This was done using two capacitors;  $C_1$  and  $C_2$ , the values of which were determined iteratively (Figure 25).

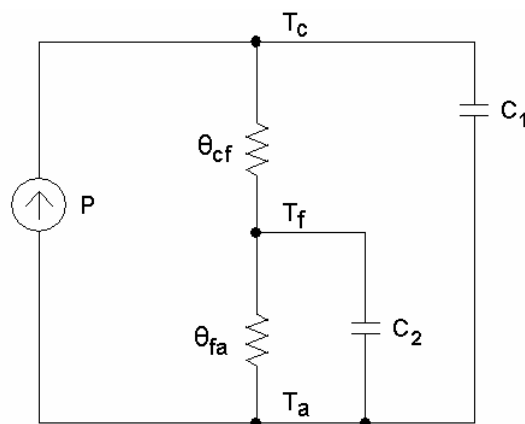


**Figure 25.** Equivalent circuit modified to account for the delay in rise time.

$T_f$ ,  $T_c$  and  $T_a$  are the temperature of the fixture, the temperature of the coil, and the ambient temperature and are represented by the voltages measured at these points in the circuit. They are also the step responses of our model, where

$$T_f(s) = \frac{P}{s} H_1(s)$$

and

$$T_c(s) = \frac{P}{s} H_2(s).$$

Both  $C_1$  and  $C_2$  are used to model the temperature rise time. For a full calculation, see Appendix B. When modelling the temperature for BEST 90,  $C_1$  was set to 0.5 F and  $C_2$  was set to 2.5 F.

In order to compare the model to the real measurements,  $T_f$  and  $T_c$  were plotted together with measurement data in MATLAB<sup>®</sup> (Figure 26).

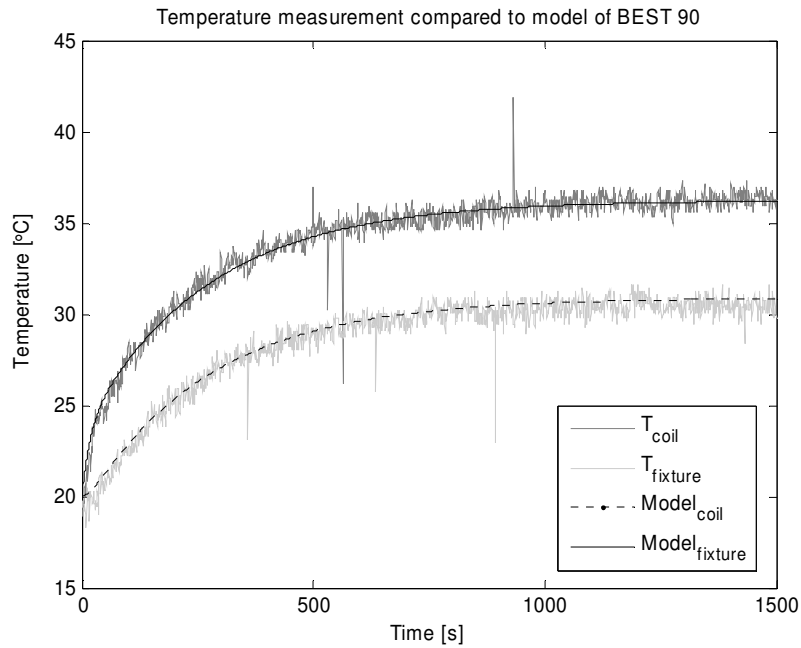


**Figure 26.** Temperature measurement of BEST 90 compared to the modelled temperature development.  $U = 1.5 \text{ V}_{\text{rms}}$   $f = 100 \text{ Hz}$

#### 4.1.5 Thermal resistance in skull bone

When measuring the thermal resistance of the dry parietal bone, similar temperature curves as for when measuring the thermal resistance within the transducer were produced. Measurements were made at 3 mm and 5 mm thick dry skull bone. An assumption that the thermal resistance varies linearly with respect to the thickness was made. The values presented are transformed to fit a piece of skull bone with a thickness of 1 cm. An example of the temperature

rise curve can be seen in Figure 27. The resulting values for the thermal resistance are plotted in Figure 28.

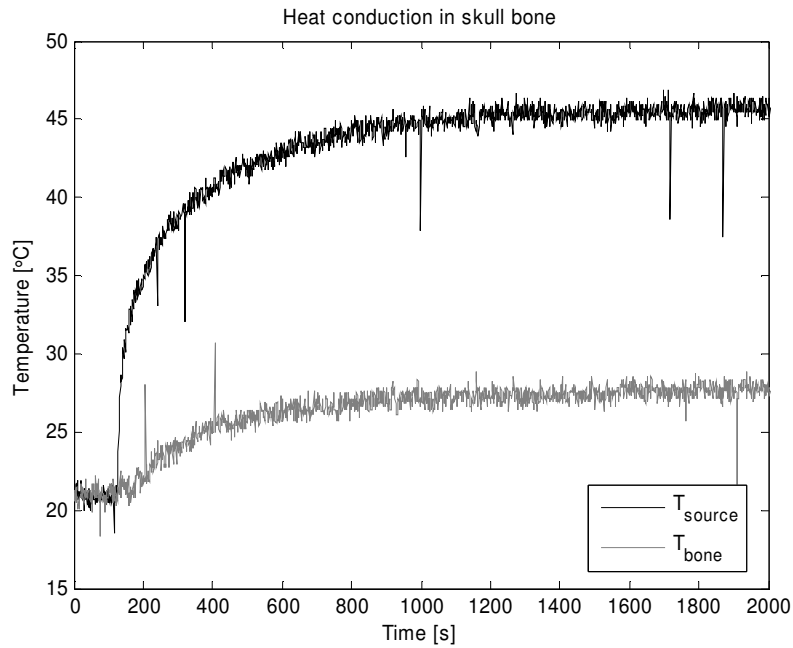


**Figure 27.** Temperature measurement of a 5 mm thick piece of dry skull bone.  $U = 10$  V, corresponds to 370 mW.

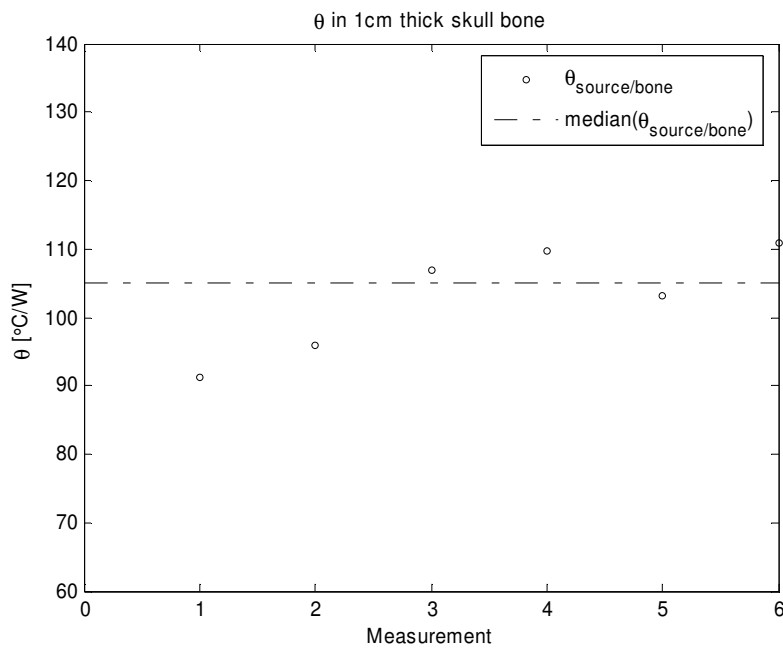
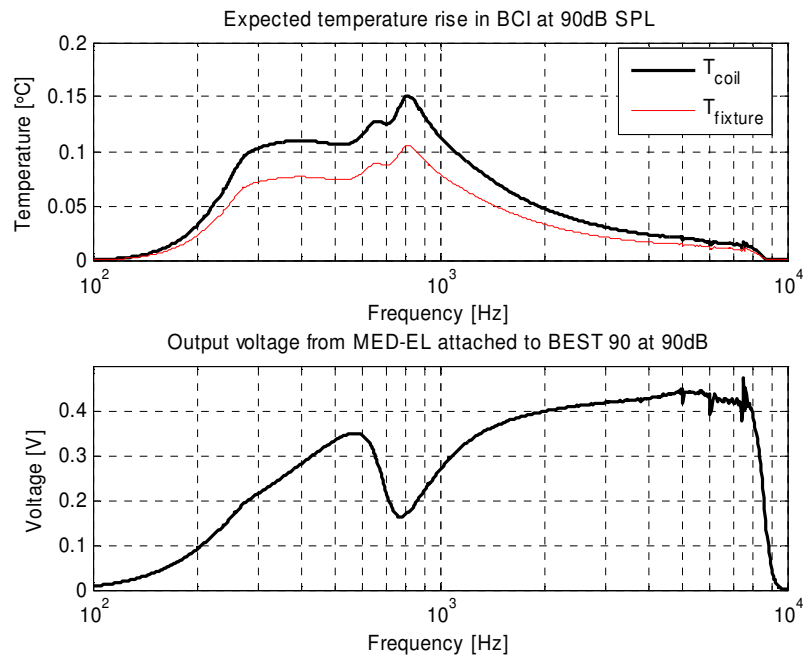


**Figure 28.** Thermal resistance for the dry skull bone at 1 cm.

As seen the  $\theta$ -value for the bone is approximately  $100^\circ\text{C/W}$ . This is in the range of the  $\theta$ -value for  $\theta_{\text{fa}}$  for the transducer.

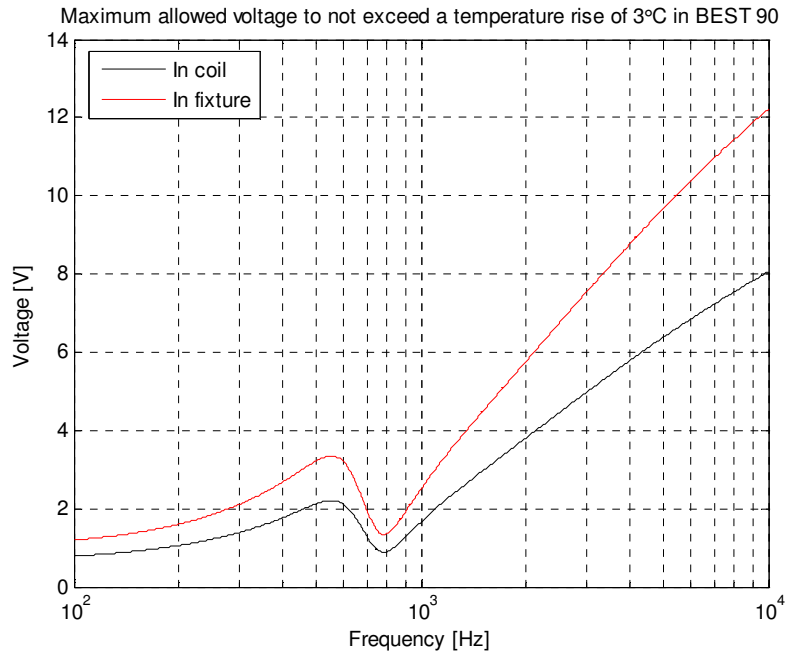
#### 4.1.6 Temperature expectations using temperature model

The temperature model can be used to calculate the expected temperature rise in the BEST transducer when a certain voltage is applied. Figure 29 shows the expected temperature rise of the BCI when the sound pressure by the microphone is at 90 dB SPL.  $\theta_{fa}$  and  $\theta_{cf}$  are  $90^{\circ}\text{C}/\text{W}$  and  $40^{\circ}\text{C}/\text{W}$  respectively.



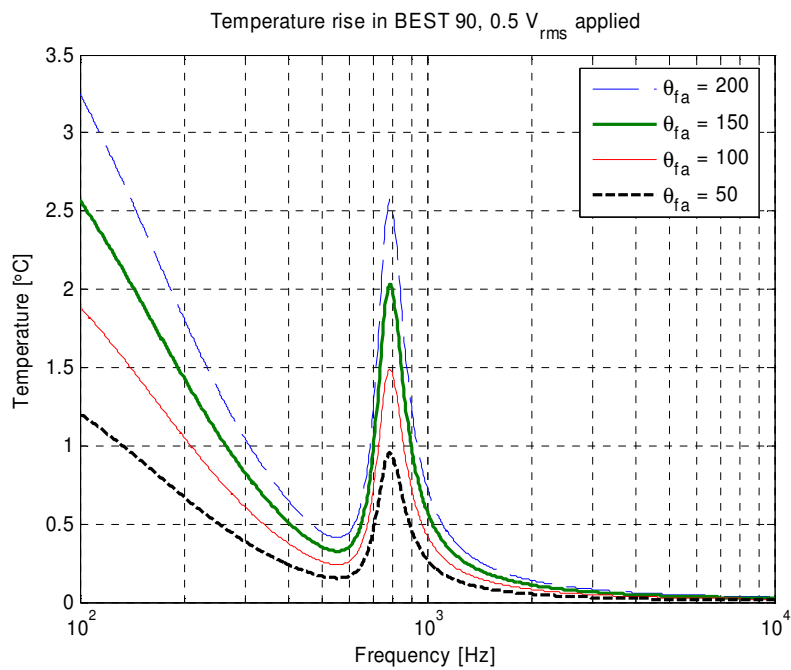
**Figure 29.** Expected temperature rise in the BCI at 90dB SPL. Output voltage from the MED-EL system [15] plotted for comparison.

The temperature model can also be used to approximate what maximum voltage can be applied to the BEST 90 without exceeding a certain temperature limit. Figure 30 shows that maximum voltage when the temperature limit is set to a three degree rise.



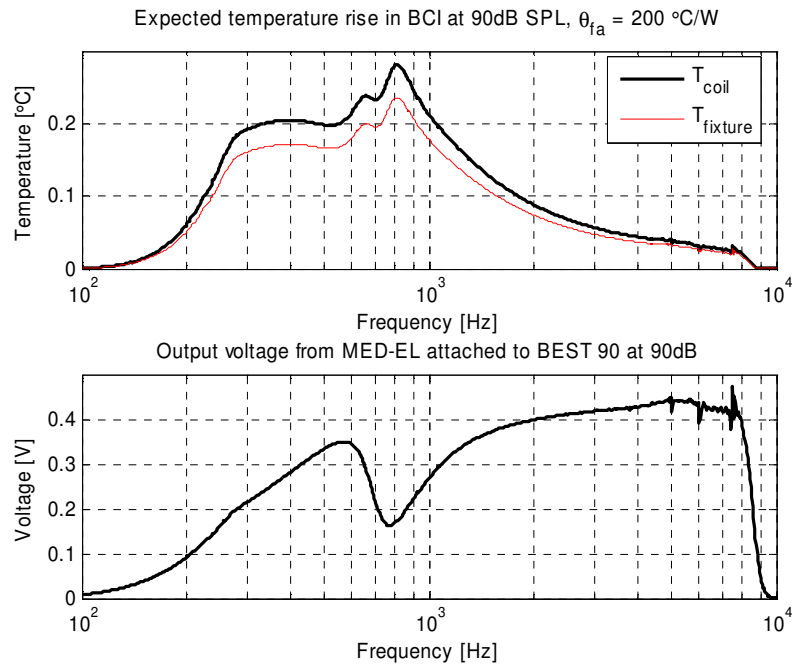
**Figure 30.** Maximum voltage that can be applied to the BEST 90 transducer before exceeding a temperature rise of 3°C at the fixture.

Figure 31 below is to show how different  $\theta$ -values affect the temperature rise in the coil.



**Figure 31.** Temperature rise in the coil when an input voltage of 0.5 V is applied.  $\theta_{cf} = 40^\circ\text{C}/\text{W}$ .

Using the temperature model with  $\theta_{fa} = 200^\circ\text{C/W}$  can give us the temperature development when the transducer is more isolated than in open air. Figure 32 shows the expected temperature rise in the BCI at 90dB.



**Figure 32.** Expected temperature rise in the BCI at 90 dB SPL.  $\theta_{fa}$  and  $\theta_{cf}$  are  $200^\circ\text{C/W}$  and  $40^\circ\text{C/W}$  respectively.

Figure 33 shows the maximum allowed voltage that can be applied to the transducer without damaging the coil wires or other components of the transducer.

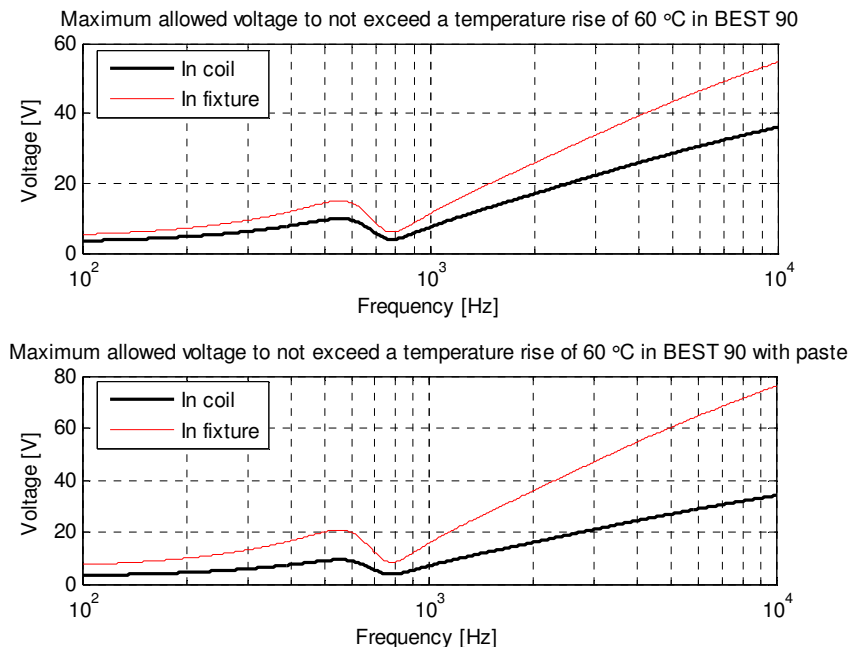


**Figure 33.** Maximum allowed voltage to be applied to the BEST 90 transducer in order to not exceed a temperature of  $80^\circ\text{C}$  with an ambient temperature of  $20^\circ\text{C}$ .  $\theta_{fa}$  and  $\theta_{cf}$  are  $90^\circ\text{C/W}$  and  $40^\circ\text{C/W}$  respectively for BEST 90 without thermally conductive paste and  $100^\circ\text{C/W}$  and  $20^\circ\text{C/W}$  for BEST 90 with thermally conductive paste.

Using voltages below these values should not damage the transducer.

#### 4.1.7 Temperature at maximum input

Results show that a significant rise in temperature is achieved at the defined maximum input. Tables 5, 6 and 7 summarize these measurements. The temperature was not allowed to reach much more than 80°C at the coil. This corresponds to a fixture temperature of approximately 60°C according to the model in 4.1.4.

##### VIBRATOR: 723- 4

Frequency [Hz]	THD [%]	Output [dBV <sub>rms</sub> ]	Input [dBV <sub>rms</sub> ]	T <sub>o</sub> [°C]	T <sub>i</sub> [°C] (after 20 min.)	T <sub>c</sub> [°C]
250	5.5	-13.9	-3.28	22	22	32
500	5.6	-15.8	4.4	22	40	58
750	5.5	-15.3	7.77	36	57	82
1000	4.5 *	-12	12	28	60 **	86
1500	1.9 *	-15.3	12	20	64 ***	92
2000	0.6 *	-19.8	12	30	41	60
3000	0.43 *	-26.6	12	30	34	49
4000	0.2 *	-32	12	25	29	42
6000	0.53 *	-48	12	24	26	38
8000	0.36 *	-48.3	12	24	26	38

\* Input voltage 4V

\*\* terminated after 5 minutes

\*\*\* terminated after 10 minutes

**Table 5.** Maximum input measurements for BEST 90-1.

##### VIBRATOR: 723- 5

Frequency [Hz]	THD [%]	Output [dBV <sub>rms</sub> ]	Input [dBV <sub>rms</sub> ]	T <sub>o</sub> [°C]	T <sub>i</sub> [°C] (after 20 min.)	T <sub>c</sub> [°C]
250	5.5	-18.8	-8.1	22	22	32
500	5.5	-19.7	0	22	25	36
750	5.5	-18.8	2	23	27	39
1000	5.5	-18.2	4.9	21	29	42
1500	3.3 *	-22	12	23	60 **	87
2000	0.8 *	-25.9	12	27	42	61
3000	0.22 *	-31.9	12	21	33	48
4000	0.64 *	-34.5	12	21	30	43
6000	0.92 *	-49	12	21	25	36
8000	0.4 *	-53	12	22	25	36

\* Input voltage 4V

\*\* terminated after 15 minutes

**Table 6.** Maximum input measurements for BEST 90-2.

**VIBRATOR: 723-3**

<i>Frequency</i> [Hz]	<i>THD</i> [%]	<i>Output</i> [dBVrms]	<i>Input</i> [dBVrms]	<i>T0</i> [°C]	<i>Tf</i> [°C] (after 20 min.)	<i>Tc</i> [°C]
250	5.5	-11.3	0.63	21	28	31
500	5.5	-17.7	2	25	31	35
750	5.5	-17.8	4.1	25	31	35
1000	5.5	-16.5	7.4	25	36	43
1500	2.8 *	-21.8	12	25	60 **	77
2000	0.7 *	-24.8	12	21	42	51
3000	0.13 *	-30	12	22	34	40
4000	0.32 *	-33.3	12	21	28	31
6000	0.43 *	-47.7	12	21	25	27
8000	0.67 *	-50.9	12	22	26	28

\* Input voltage 4V

\*\* terminated after 10 minutes

**Table 7.** Maximum input measurements for BEST 90-3.



## 4.2 Cadaver head investigations

The implant stability was measured afterwards using RFA technique and was found to be satisfactory greater than ISQ = 80.

### 4.2.1 Frequency response with constant electrical stimulation

The ipsilateral frequency response for the BEST transducer in position A and in position B is shown in Figure 34.

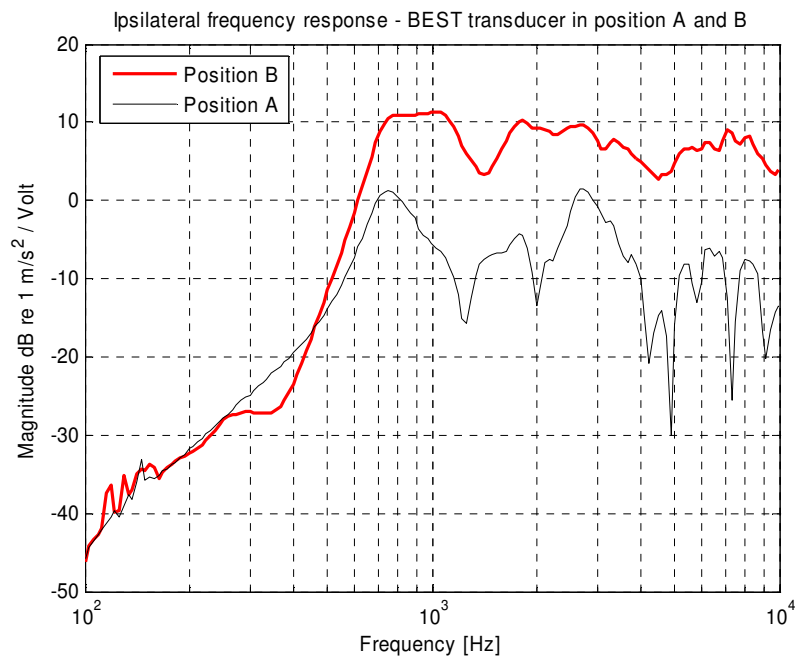


**Figure 34.** The ipsilateral frequency response at a constant input voltage level of 500 mV. Comparison of the BEST transducer in position A and in position B.

The response is 10-15 dB higher for frequencies between 650 Hz - 10 kHz with the BEST in position B compared to position A.

The contralateral frequency response for the BEST transducer in position A and in position B is shown in Figure 35.

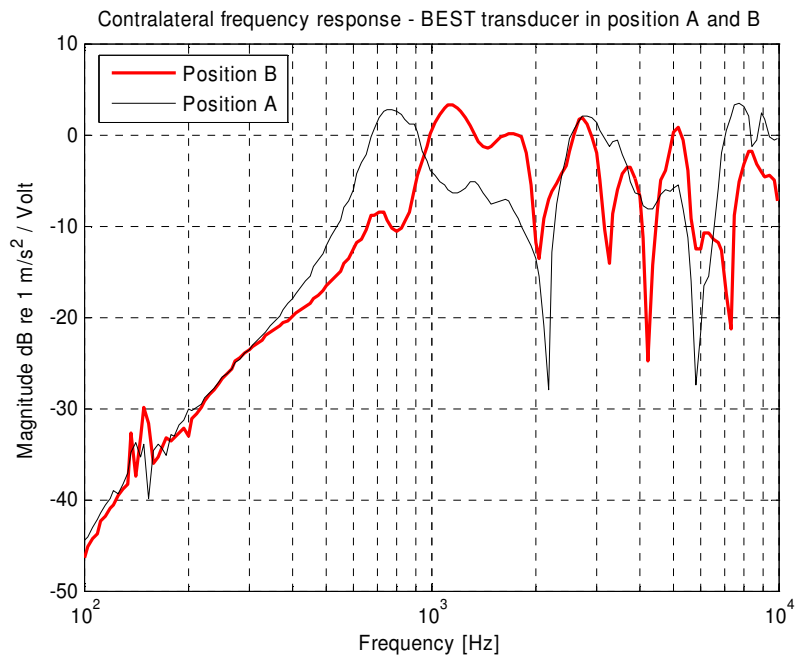


**Figure 35.** The contralateral frequency response at a constant input voltage level of 500 mV. Comparison of the BEST transducer in position A and in position B.

Compared to the ipsilateral response, 10 dB has been lost in the response from position B and the maximum amplitude is reached at 1.2 kHz instead of in the range 750-1100 Hz. There are no significant differences between the ipsilateral and the contralateral response from position A.

Figure 36 shows the ipsilateral frequency response for the BAHA transducer in position A and in position B at a constant input voltage of 500 mV.

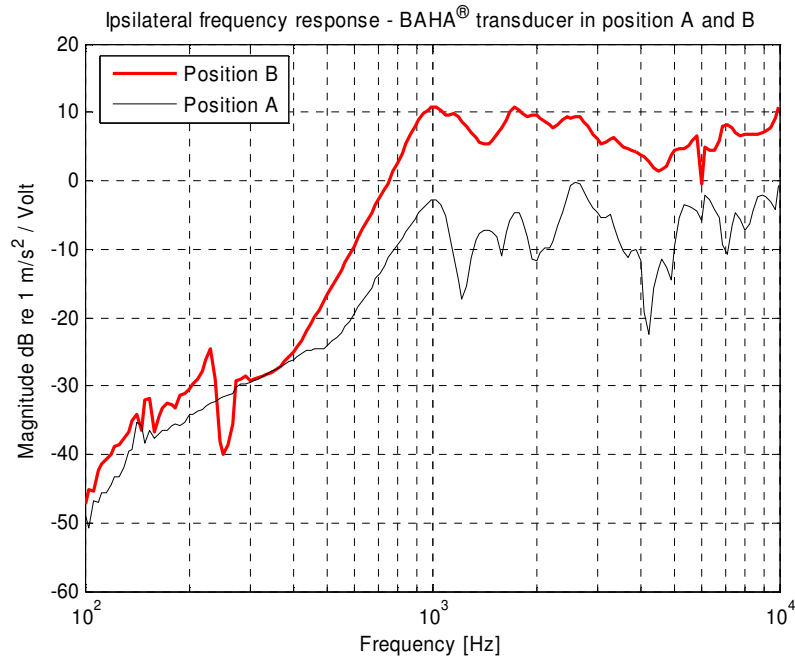


**Figure 36.** The ipsilateral frequency response for the BAHA transducer at a constant input voltage level of 500 mV.

The response is higher when the transducer is placed in position B than when it is placed in position A.

The contralateral frequency response for the BAHA transducer is presented in Figure 37.

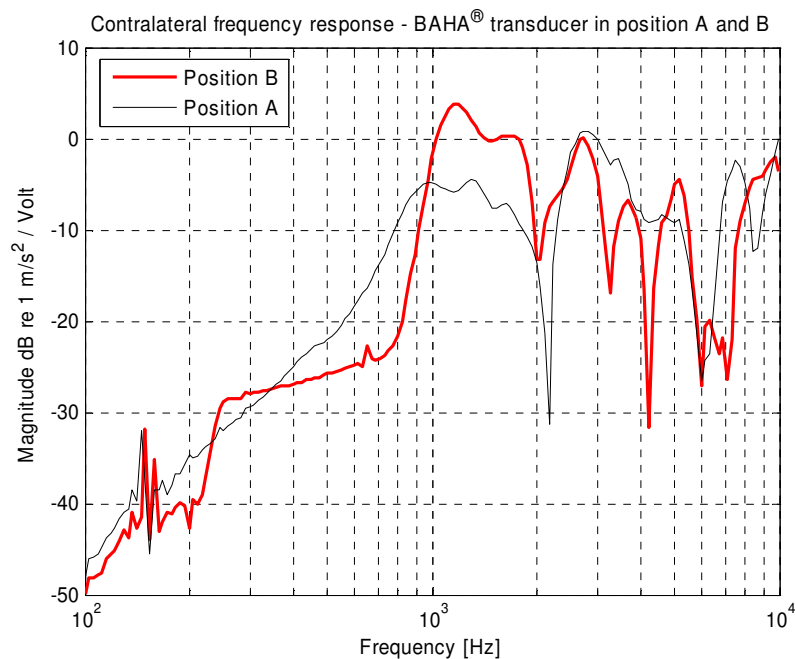


**Figure 37.** The contralateral frequency response for the BAHA transducer at a constant input voltage level of 500 mV.

## 4.2.2 Sound pressure output response and total harmonic distortion

The sound pressure at the reference microphone obviously changed whenever an object was moved, so new equalising curves needed to be recorded after each change of the set-up. However, an example of the sound pressure at the reference microphone following a 90 dB SPL output from the speaker input signal is presented in Figure 38 below.

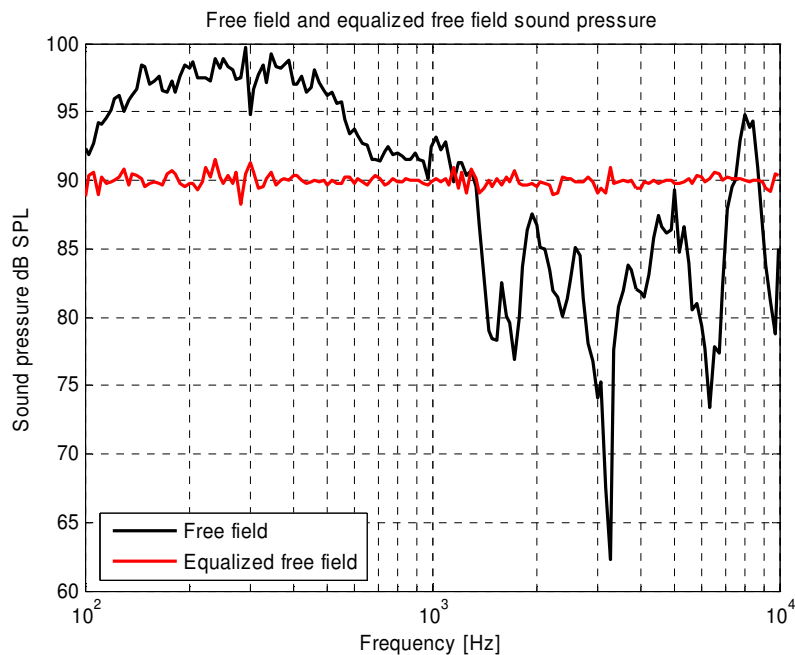


**Figure 38.** The free field sound pressure at the reference microphone before and after equalization.

This clearly shows how complex the test environment was. The characteristics of the room made the sound pressure level vary with up to 35 dB. The sound pressure level at the reference microphone after equalization can be seen in the same Figure. The variations in SPL are now less than 3 dB, which was considered to be sufficient.

The ipsilateral output response and the distortion of the BCI in position B is presented in Figure 39. The distortion is measured at 70 dB SPL.

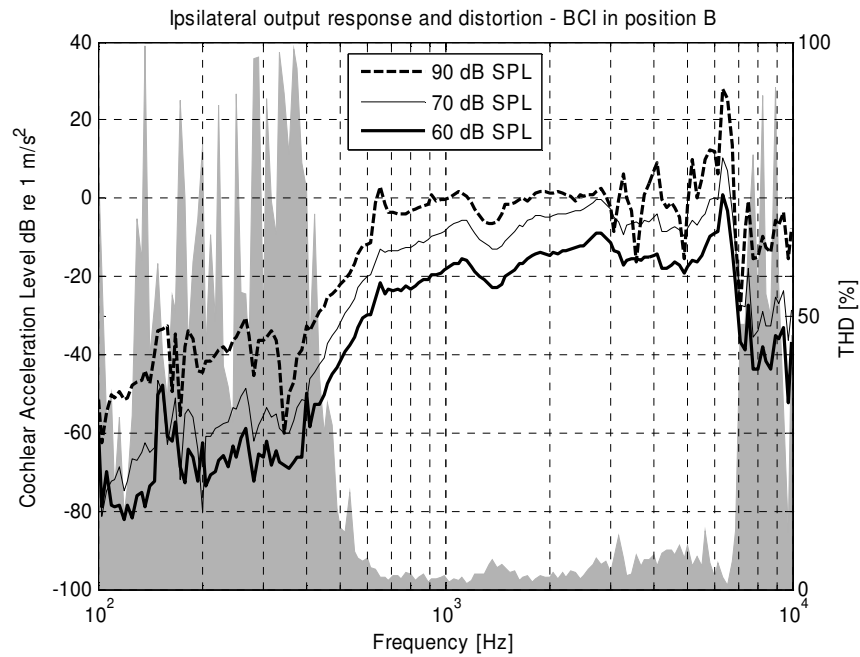


**Figure 39.** Sound pressure output response from the BCI in position B measured at the ipsilateral side. The corresponding THD at 70 dB is plotted in grey in the background.

The contralateral output response and distortion of the BCI in position B is shown in Figure 40 below.

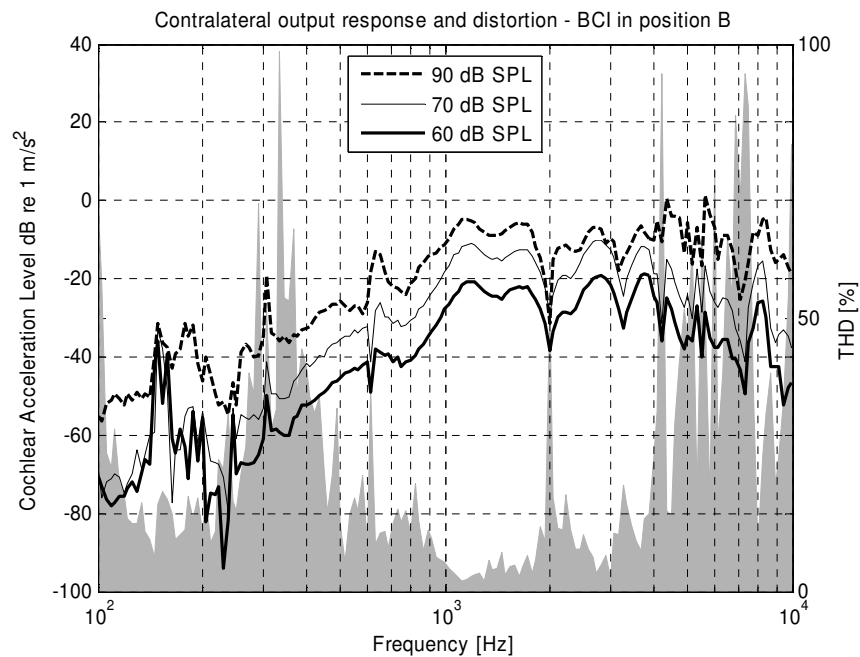


**Figure 40.** Sound pressure output response from the BCI in position B measured at the contralateral side. The corresponding THD at 70 dB is plotted in grey in the background.

The difference between the ipsilateral and the contralateral output response from position B is within 10-15 dB measured at 60 dB SPL throughout the spectra. The only major exception is found at the 2 kHz antiresonance, where there is a sudden dip in the contralateral response. Another notable difference is that the contralateral response reaches its maximum at 1 kHz whereas the ipsilateral response reaches its maximum at 650 Hz.

The ipsilateral output response from BAHA in position A can be seen in Figure 41.

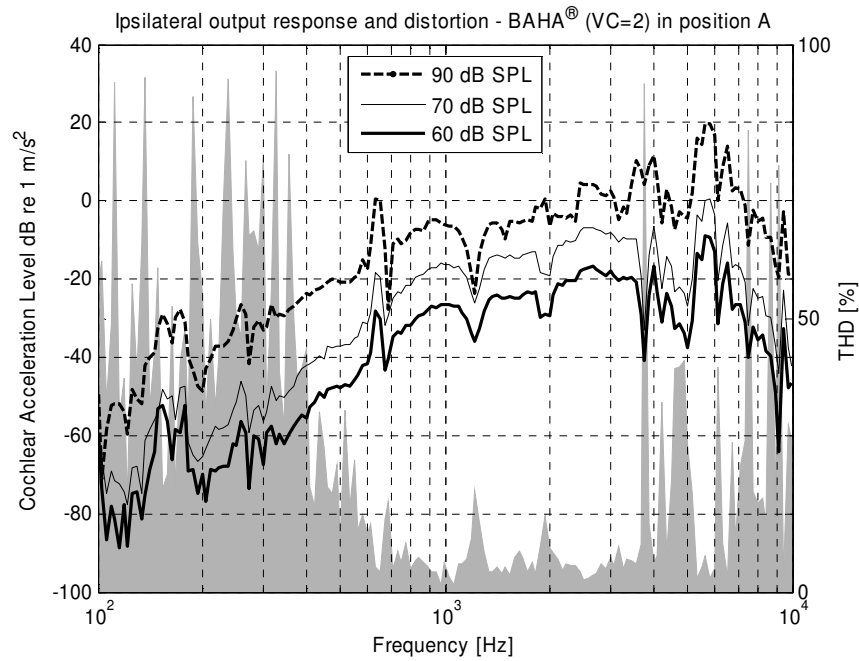


**Figure 41.** Sound pressure output response from the BAHA-device in position A measured at the ipsilateral side. The corresponding THD at 70 dB is plotted in grey in the background.

The contralateral output response from BAHA in position A can be seen in Figure 42.

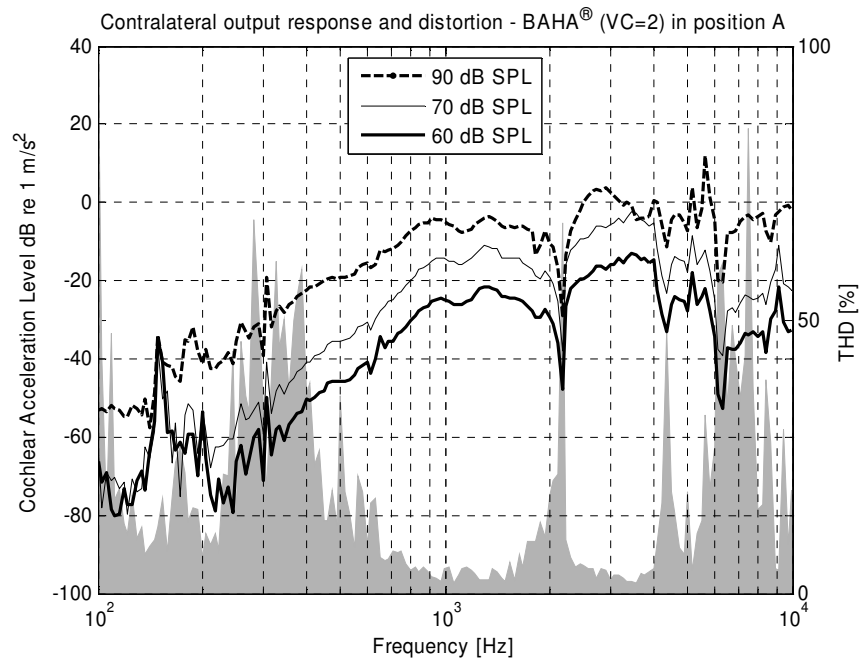


**Figure 42.** Sound pressure output response from the BAHA-device in position A measured at the contralateral side. The corresponding THD at 70 dB is given in the background.

The dip at 2.2 kHz can be seen in the BCI output response for the contralateral side as well, but at 2 kHz.

## 4.2.4 Input impedance of BAHA

The input impedance of the BAHA can be seen in Figure 43 below.

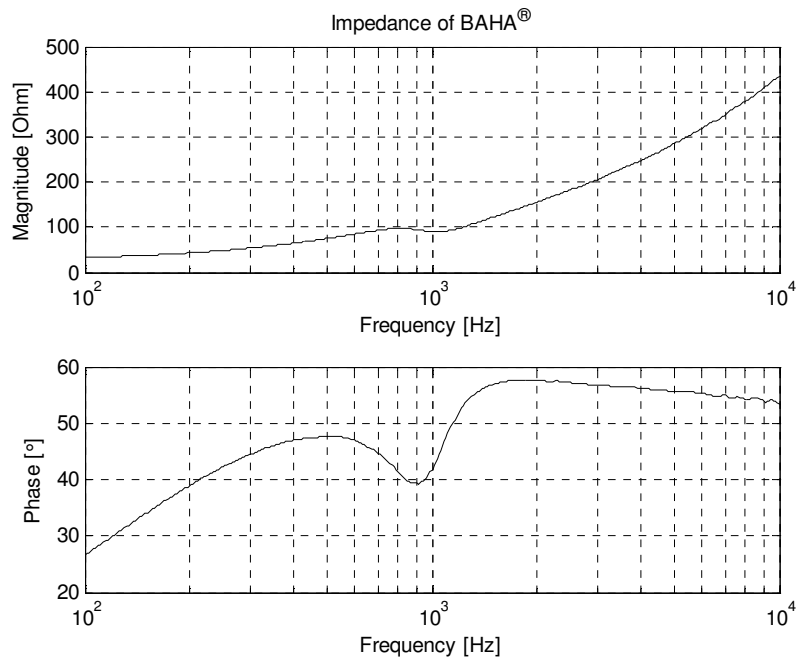


**Figure 43** Input impedance magnitude and phase of Baha® 300 Classic transducer.



## 5. Discussion

### 5.1 Thermal resistance

First of all it is worth noting that most of the results for  $\theta_{fa}$  are rather crude, since the ambient temperature was measured using a conventional fluid thermometer. Though, it is not the heat conduction between the fixture and the surrounding air that is most important. Instead, it is far more interesting to know how much heat will be conducted from the transducer coil to the external fixture. That fixture will provide a contact point with the skull bone when implanted, and will as such also provide a path for heat to be lead away to the bone. Remembering that the bone tissue can not tolerate temperatures that are too high, one will see why it is important to know the temperature of the fixture. This thesis has established means of deciding the fixture temperature as a function of input power. To further evaluate if the BEST is suitable for implantation, one would need to perform cadaver head investigations of how heat is distributed around the implantation site in the skull bone. One has to take in consideration that, when completely isolated inside the skull, the temperature rise within the BEST and consequently in the implantation site might be much higher. This would be because there are no external means of cooling the transducer. If, for instance, the bone around the transducer is thermally isolating, there is nowhere for the heat to go, and the bone's ability to transport heat away is not enough. However if there are blood vessels near the implantation site this might be enough to cool the transducer.

When making temperature measurements at higher frequencies (above 4 kHz) for BEST 90, there was severe noise at the input levels that were tested. Therefore it was decided to avoid measuring temperature at those frequencies and input voltages. With lower input voltage no temperature rise could be detected at all. Later on it was discovered that the noise might originate from the thermocouples, since the vibrations from the transducer were transmitted onto them. However, we concluded that the lack of measurements at higher frequencies would not affect the final results or conclusions, since the input voltages at those frequencies were much higher than what would be expected at normal operating conditions.

For BEST 90 the calculated median values for  $\theta_{fa}$  and  $\theta_{cf}$  was  $90^{\circ}\text{C}/\text{W}$  and  $40^{\circ}\text{C}/\text{W}$  respectively. The  $\theta_{fa}$  and  $\theta_{cf}$  for BEST 90 with paste was  $100^{\circ}\text{C}/\text{W}$  and  $20^{\circ}\text{C}/\text{W}$  respectively. Comparing these values it is noted that the value of  $\theta_{cf}$  for the BEST with thermally conductive paste has been decreased into half the size of  $\theta_{cf}$  for the BEST without paste. As expected the heat in the coil was more efficiently led away when thermally conductive paste was inserted between the coil and the external fixture. When reviewing the measurements for BEST 90 with thermally conductive paste, the temperature at the external fixture was increased, however, the coil temperature remained more or less the same.

Moving on to the results for BEST 150, it was noted that this device requires less power to yield the same temperature as the BEST 90 because of the lower input impedance (see Figure 15 in section 4.1.1). The first measurements at DC and low AC frequencies (up to 200 Hz) showed some consistency for  $\theta_{fa}$  and  $\theta_{cf}$ . For frequencies between 200 Hz and 600 Hz,  $\theta_{cf}$  seemed to drop off linearly as can be seen in Figure 20.  $\theta_{fa}$  show some variability, 0,8V and 0,7V do not give the same value. For all frequencies  $\theta_{fa}$  shows less consistency and more variations than  $\theta_{cf}$ . Given that the variations are present at all frequencies and given that it is the thermal resistance value between the fixture and ambient, it is possible to assume that these 'errors' are caused by the crude measure of the ambient temperature. On the other hand, one would expect to see similar variations in  $\theta_{fa}$  for BEST 150 with thermally conductive paste. This, however is not the case, the different  $\theta_{fa}$  are more or less the same at each frequency. This could be explained by noting that the temperature on the fixture was increased when applying paste between the transducer coil and the external fixture. An increased temperature implies that the difference between fixture and ambient temperature is greater and may therefore also improve the accuracy of the resulting  $\theta_{fa}$ .

For  $\theta_{cf}$  this does not appear to be significant. What is significant for  $\theta_{cf}$  however, are the values at 300 Hz, where all measurements give different results. At frequencies above 400 Hz the heat development in the transducer is so small at voltages below distortion level, that  $\theta_{cf}$  grows very little, and is even negative. This effect is reversed at some point as can be seen at 1000 Hz in Figure 22.

As expected for BEST 150 with thermally conductive paste, the temperature measured on the external fixture was increased; however, the coil temperature remained more or less the same. This implies that  $\theta_{fa}$  increases and  $\theta_{cf}$  decreases. It seems that  $\theta_{cf}$  for some reason increases for higher frequencies (Figure 23). The median values have been calculated using the values from 0 - 1.5 kHz.

For the B71 it seems that  $\theta_{cf}$  decreases for higher frequencies (Figure 24). The median values have been calculated using the values from 0 - 1 kHz. The temperature rise in the B71 was in general lower than for the BEST transducer when applying the same amount of power. This can probably be explained by the fact that the B71 has a much higher mass and size of housing which can absorb a greater amount of heat than the BEST transducer.

When using the temperature model with the calculated  $\theta$ -values it was found that the temperature development in the BEST transducer is relatively low in clinical applications. When applying as much as 1 V<sub>rms</sub> there is a temperature rise of only 3°C. It should be noted that this temperature rise will occur only if the signal to the transducer is constant for approximately ten minutes because of the rise time.

The thermal resistance of the skull bone at the possible implant site should be measured in a cadaver head in order to obtain a more accurate value. The measurements presented in this thesis were only supposed to give a rough idea of the range in which the thermal resistance of skull bone lies.

## **5.2 Output response**

The acoustics of the room where the measurements were made displayed large differences between different frequencies. With PULSE the room SPL could be fairly well equalized and so there are no reasons to believe that the differences in the sound pressure during a measure had a major influence on the results.

The ipsilateral output response from the BCI in position B, see Figure 39, shows linearity up to 80 dB SPL. It reaches its maximum at 700 Hz which is due to the resonance frequency of the BEST. The distortion is approximately 2-5 % in the range between 600 Hz to 6.5 kHz at 70 dB SPL.

The huge dip at 2 kHz seen in the contralateral output response from the BCI in position B, Figure 40, is believed to be caused by antiresonances in the skull. One might expect that it is a consequence of the complex acoustics of the room, however looking at the contralateral plots of the electrical frequency response for the BEST transducer, (Figure 35); similar dips can be seen in close proximity to 2 kHz. Given that the stimulus in these measurements was not sound pressure, but rather a constant amplitude frequency sweep electrical input, it is highly unlikely that the dips are due to room acoustics. In favour of that assumption, one can also argue that no such dips can be seen in any of the ipsilateral measurements, as they should if the room had had any influence on that. The maximum of the output response is reached at 1.1 kHz.

Both the ipsilateral and the contralateral output responses from the Baha<sup>®</sup> Classic 300 in position A are linear up to almost 90 dB SPL. The distortion is slightly higher than the distortion of the BCI.

When comparing ipsilateral output responses from the BCI in position B and the Baha<sup>®</sup> Classic 300 in position A, it is noticed that the BCI gives a higher output response than the Baha<sup>®</sup> Classic 300 for frequencies between 700 Hz and 2 kHz. The peak at 650 Hz might be caused by resonances due to the transducer being saturated. It should also be noted that the resonance frequency of the BEST transducer is located around 650 Hz, therefore it might be assumed that this peak is a consequence of that.

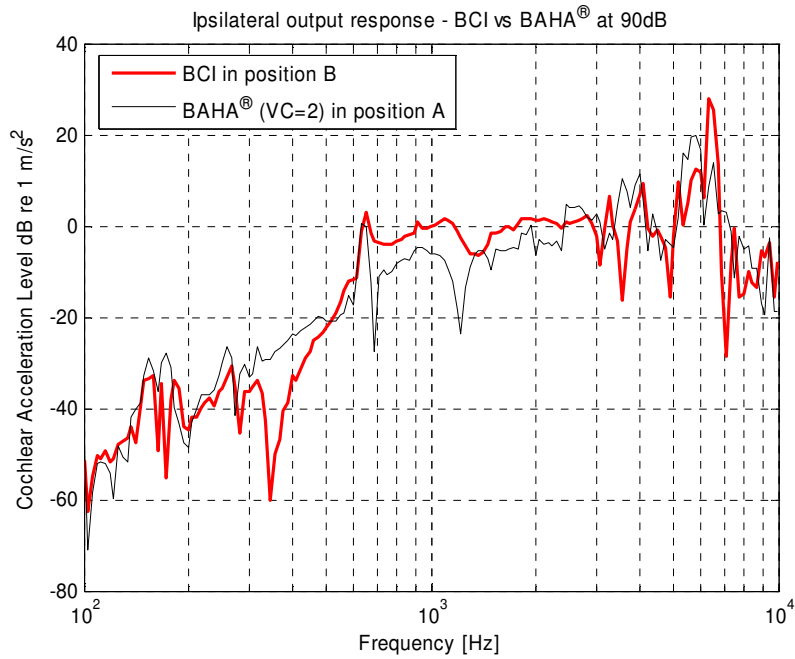


**Figure 44.** Comparison of the sound pressure output response at 90 dB SPL from the BCI in position B and the Baha® Classic 300 in position A measured on the ipsilateral side.

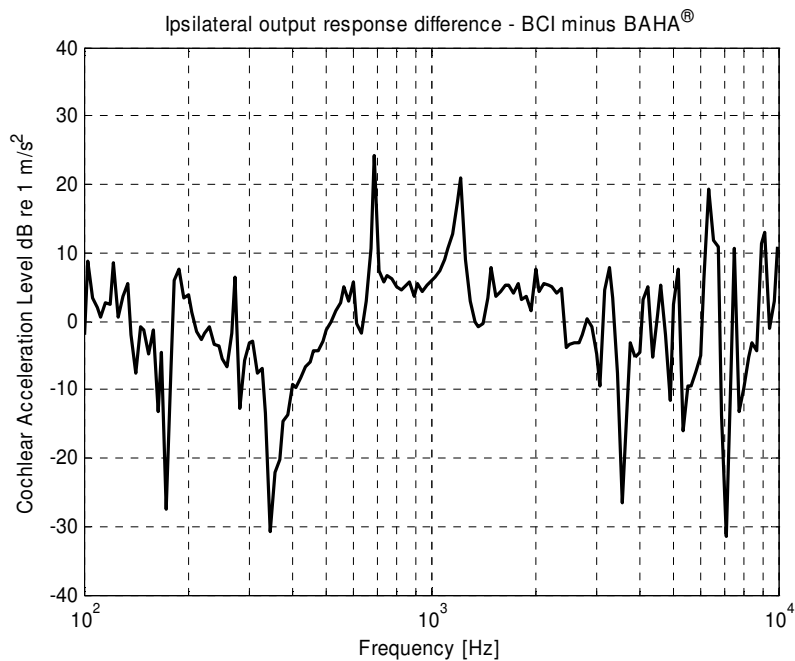


**Figure 45.** Difference of ipsilateral maximum output acceleration level at 90 dB SPL between the BCI and Baha® Classic 300.

The BCI gives a slightly higher response, approximately 5 dB, compared to the Baha® Classic 300 for frequencies in the range of 700 Hz to 2 kHz.

A comparison of the contralateral output response at 90 dB between BCI in position B and the Baha<sup>®</sup> Classic 300 in position A is presented in Figure 46.

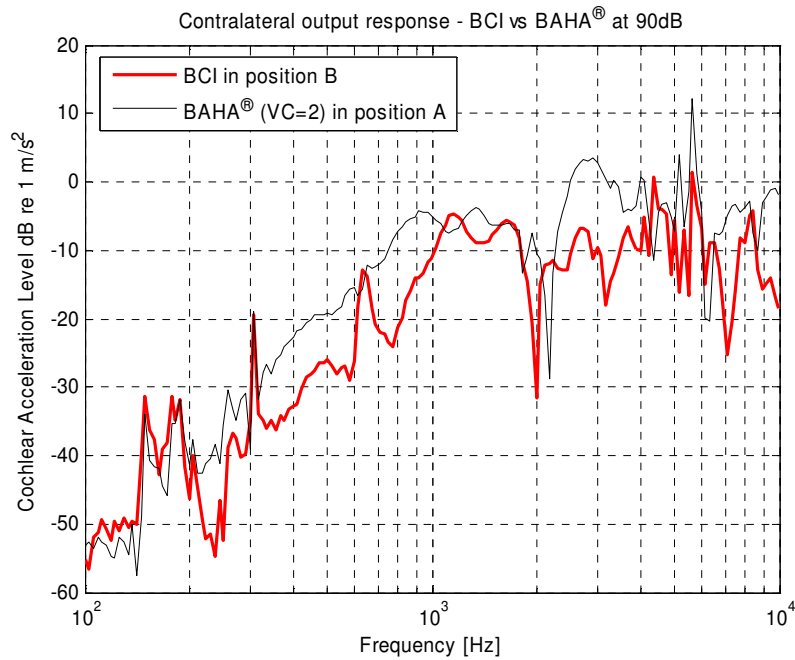


**Figure 46.** Comparison of the contralateral sound pressure output response at 90 dB SPL from the BCI in position B and the Baha<sup>®</sup> Classic 300 in position A.

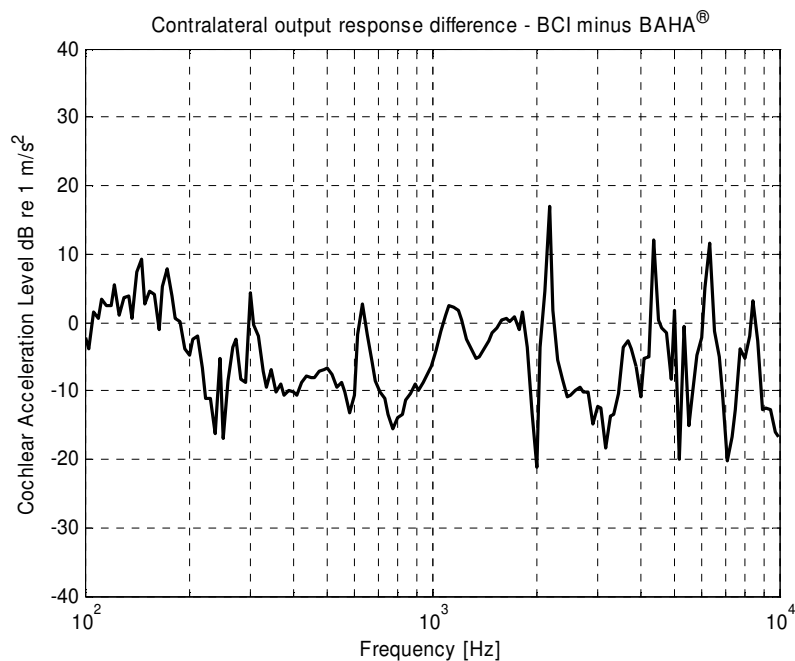


**Figure 47.** Difference of contralateral maximum output acceleration level at 90 dB SPL between the BCI and Baha<sup>®</sup> Classic 300.

It is noticed that the Baha<sup>®</sup> Classic 300 has a significantly higher response, 10 dB, for frequencies between 300 Hz - 1 kHz. It is assumed that this is a consequence of the path of vibrations in the skull. That path indicates that stimulation in position A should produce a higher contralateral response than stimulation in position B.

It is of interest to compare the measurements on the cadaver with measurements made on a dry and semi dry skull in order to see if there are any significant differences. If no major differences are found one can continue testing bone transducers on a semi dry skull and still have fairly accurate results. Figure 48 shows the output responses at 90 dB SPL for cadaver, dry and semi dry skull. The data output response from the dry and semi dry skull are taken from reference material [15].

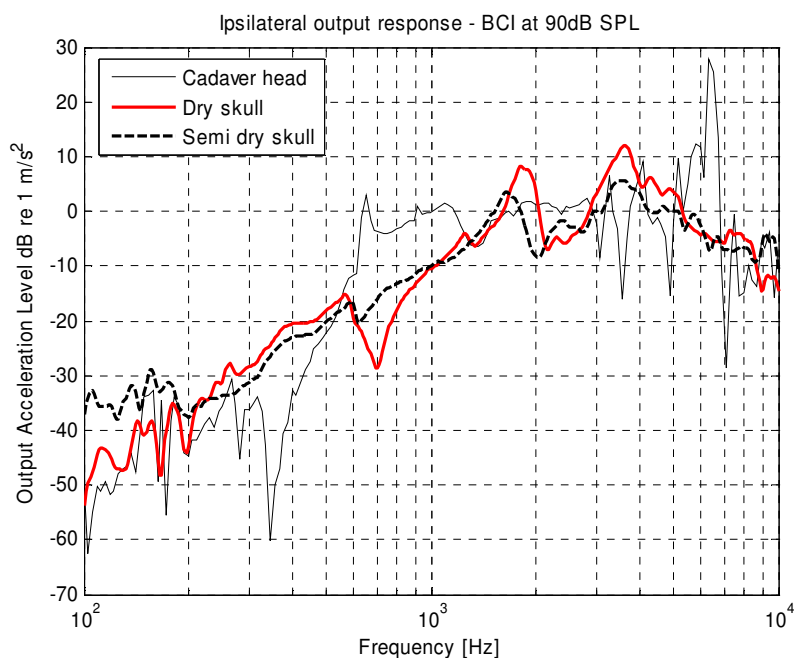


**Figure 48.** Output response from BCI in position B on cadaver, dry and semi dry skull at 90 dB SPL.

The cadaver head response is higher for frequencies between 600 Hz - 1.2 kHz and has a much steeper roll-off at the lower frequencies. This phenomenon is seen in several of our measurements independent of which transducer was used and what placement it had. It is therefore most likely a skull specific characteristic.

### 5.3 Frequency response

It is of interest to compare the ipsilateral response from the BEST transducer in position B to the ipsilateral response from the BAHA in position A. A plot of both curves can be found in Figure 49.

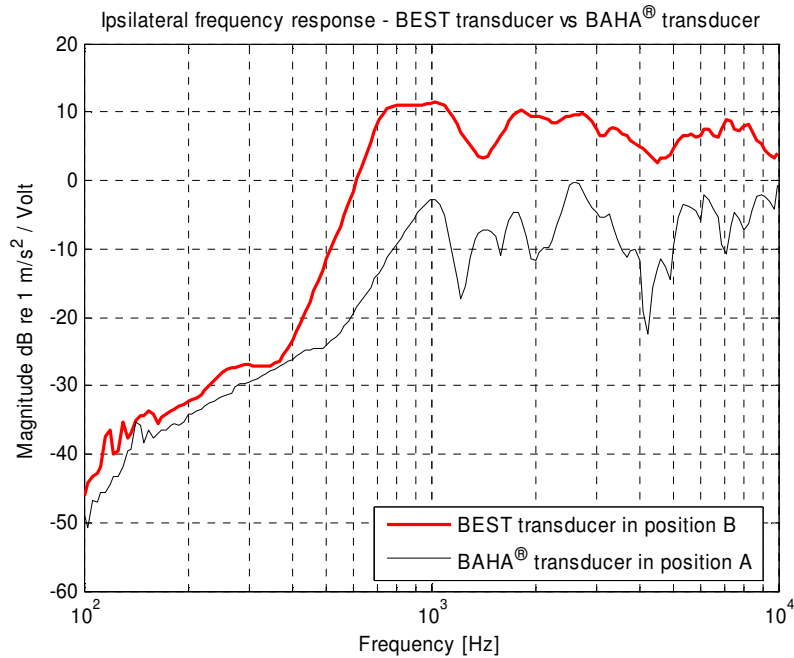


**Figure 49.** The ipsilateral frequency response at a constant input voltage level of 500 mV. Comparison of the BEST transducer in position B and the BAHA transducer in position A.

The difference between the BEST transducer in position B and the BAHA transducer in position A is 10-20 dB for frequencies between 500 Hz - 8 kHz. The difference is significantly higher than for the output response between the BCI in position B and the BAHA in position A. The response from the BEST is smoother with less dips. This result might indicate that position A involves more skull resonant phenomena than position B.

A comparison between the contralateral responses is also of interest to see how well the BEST transducer in position B can transfer the vibrations of the bone compared to the BAHA transducer in position A. Figure 50 shows this comparison.

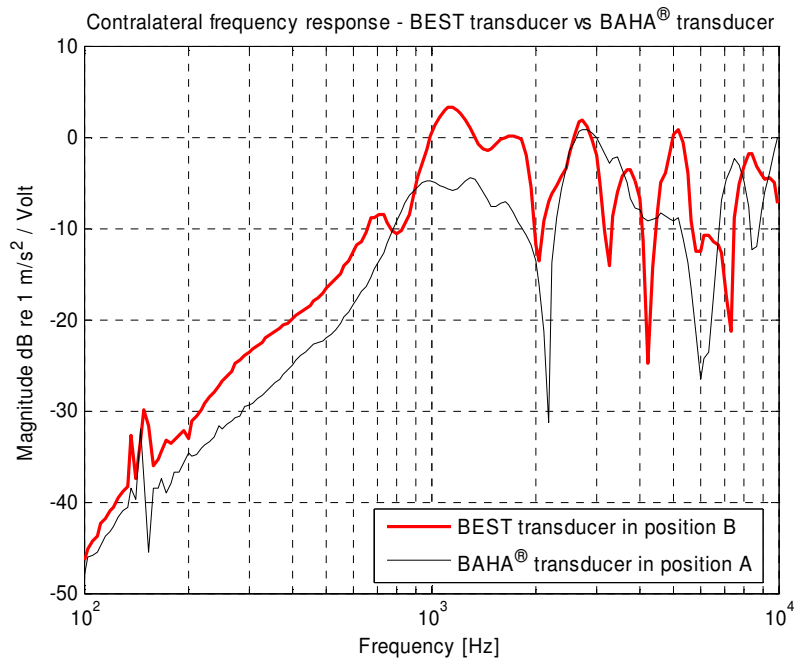


**Figure 50.** The contralateral frequency response at a constant input voltage level of 500 mV. Comparison of the BEST transducer in position B and the BAHA transducer in position A.

It is noticeable that the frequency response from the BEST transducer has a higher response at lower frequencies at 150 Hz - 2 kHz. This is the contrary to the output response of the BCI compared to the BAHA at 90 dB SPL as seen in Figure 46. Despite the common theory that the contralateral response should be lower from stimuli in position B rather than in position A, it is found here that the contralateral response is higher when using the BEST in position B than it is when using the BAHA in position A.



The frequency response for the dry skull, semi dry skull and for the cadaver is shown in Figure 51 below.

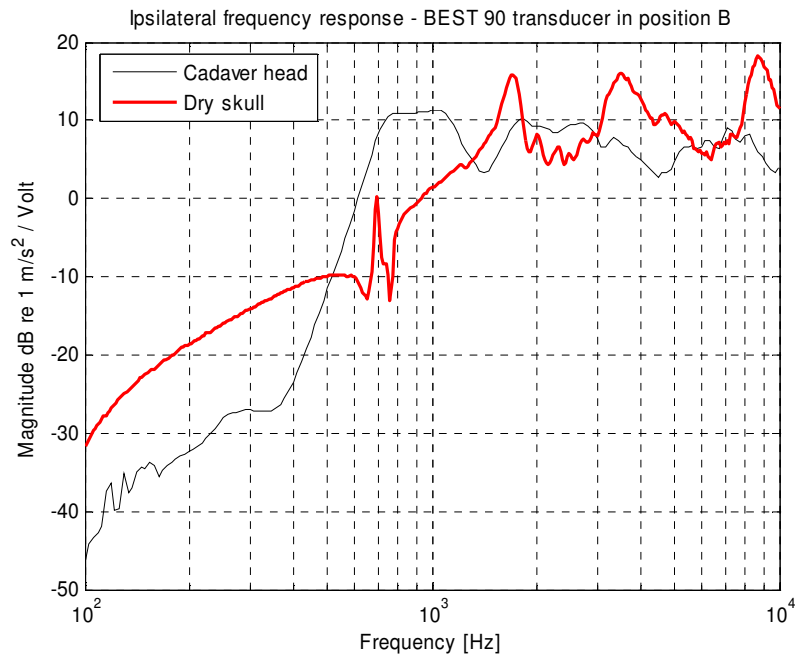


**Figure 51.** Frequency response from BEST 90 transducer in position B on cadaver and dry skull.

The response is higher for the cadaver frequency response from 500 Hz and up to 1.3 kHz. Thereafter the response is almost the same for both skulls.

Figures 34 and 36 show that a better ipsilateral frequency response is achieved when the transducer is in position B, independent of what transducer is used. The BEST transducer has reached its maximum of 10 dB at 700 Hz meanwhile the BAHA has reached its maximum of 10 dB at 1 kHz.

The frequency response is higher for the BEST transducer in position B than for the BAHA transducer in position A at lower frequencies meanwhile the output response for the BCI in position B is lower than the Baha<sup>®</sup> Classic 300 in position A. One theory is that this can be explained by looking at the maximum output voltage that the MED-EL system can give the BEST transducer in Figure 29. At maximum the MED-EL system at standard settings can give the BEST transducer 0.4 V at 90 dB SPL whereas the frequency response has been measured at 0.5 V for both the BEST transducer and the BAHA transducer. The BAHA transducer is probably getting a higher voltage than 0.4 V from its amplifier.

## 6. Conclusion

There are obvious advantages of leaving the skin intact, compared to a permanent skin penetration implant, when using a bone anchored hearing aid. This study have investigated if a transcutaneous bone conduction implant could be an alternative to the presently used percutaneous Baha<sup>®</sup> Classic 300 from a electro acoustical point of view and if the temperature rise inside the implanted transducer gets to high for human tissue.

It was found that the transcutaneous bone conduction implant, the BCI, has

- low temperature rise when it is driven by the Vibrant<sup>®</sup> Soundbridge<sup>®</sup>,
- higher ipsilateral output response than the Baha<sup>®</sup> Classic 300 at main speech frequencies,
- poorer contralateral output response than the Baha<sup>®</sup> Classic 300 at main speech frequencies.

More tests on cadaver heads must be performed to verify the results but also in vivo tests must be performed. In vivo measurements of how a temperature rise in the skull bone is dissipated are also of interest.

## References

- [1] Håkansson B., Eeg-Olofsson M., Reinfeldt S., Stenfelt S., Granström G., (2007), *Percutaneous versus transcutaneous bone conduction implant systems - a feasibility study on a cadaver head*, manuscript
- [2] VIBRANT MED-EL, <http://www.vibrantmedel.us> (Acc 2007-09-07)
- [3] Överblick av Cochlears Baha-produkter, <http://www.cochlear.se/> (Acc 2007-09-12)
- [4] Stenfelt S., Håkansson B., Tjellström A., (2000), *Vibration characteristics of bone conducted sound in vitro*, J. Acoust. Soc. Am. 107 (1), 422-431
- [5] Stenfelt S., (1999), *Hearing by bone conduction - Physical and Physiological aspects*, Department of Signals and Systems, Chalmers, ISBN 91-7197-758-9, ISSN 0346-718X
- [6] Håkansson B., (2003), *The balanced electromagnetic separation transducer - A new bone conduction transducer*, J. Acoust. Soc. Am. 113(2)
- [7] Eriksson A. R., (1984), *Heat-induced bone tissue injury: an in vivo investigation of heat tolerance of one tissue and temperature rise in the drilling of cortical bone*, Gothenburg University, ISBN 91-7222-680-3
- [8] Sedra A. S., Smith K. C., (2004), *Microelectronic circuits (5<sup>th</sup> ed.)*, Oxford University Press, ISBN 0-19-514252-7
- [9] Reinfeldt S. (2006), *Bone conducted sound transmission for communication systems*, Lic. Thesis. Chalmers University of Technology, Gothenburg, ISSN 1403-266X
- [10] Mulgrew B., Grant P., Thompson J., (2003), *Digital Signal Processing - Concepts and applications (2<sup>nd</sup> ed.)*, Palgrave MacMillan, ISBN 0-333-96356-3
- [11] Håkansson, B., PhD, Gothenburg, Personal communication, 2007
- [12] Brüel & Kjaer, <http://www.bksv.com> (Acc 2007-09-07)
- [13] Agilent Technologies, <http://www.agilent.com> (Acc 2007-09-10)
- [14] Polytec GmbH, <http://www.polytec.com> (Acc 2007-05-20)
- [15] Andersson A., Östli P., (2007), *In vitro investigation of a mastoid anchored transcutaneous bone conduction hearing system*, Master Thesis, Chalmers University of Technology, Gothenburg, manuscript

# Appendix A

## BEST 90

Unaltered				Thermally conductive paste			
<i>Frequency [Hz]</i>	<i>Input Voltage [V<sub>rms</sub>]</i>	<i>T<sub>c</sub></i>	<i>T<sub>f</sub></i>	<i>Frequency [Hz]</i>	<i>Input Voltage [V<sub>rms</sub>]</i>	<i>T<sub>c</sub></i>	<i>T<sub>f</sub></i>
0	1	29	25	0	1	30	28
0	1.5	40	34	0	1.5	39	36
0	2	53	44	0	2	51	46
100	1.5	36	31	100	1.5	37	34
200	2	40	33	100	2	50	45
400	1	21	21	200	1.5	31	29
400	2	22	22	200	2	44	40
400	2	26	25	300	1.5	29	27
4000	1	18	18	300	2	35	33
4000	2	19	19	400	2	33	32

## BEST 150

Unaltered				Thermally conductive paste			
<i>Frequency [Hz]</i>	<i>Input Voltage [V<sub>rms</sub>]</i>	<i>T<sub>c</sub></i>	<i>T<sub>f</sub></i>	<i>Frequency [Hz]</i>	<i>Input Voltage [V<sub>rms</sub>]</i>	<i>T<sub>c</sub></i>	<i>T<sub>f</sub></i>
0	1	51	41	0	1	48	43
100	1	48	40	100	1	48	44
150	0.8	38	34	200	0.8	33	31
200	0.8	33	29	300	0.8	29	28
250	0.8	31	29	400	0.8	26	26
300	0.8	29	27	500	0.6	26	26
350	0.8	26	25	1000	1.8	37	35
400	0.8	25	25	2000	2.4	31	30
500	0.6	25	26	3000	2.8	29	29
600	0.6	29	27	4000	3.4	30	30
700	1	33	29	1500	1.8	30	29
800	1	30	28	2500	2.4	28	27
900	1.5	36	32	3500	3.4	31	30
1000	1	27	26				
1000	1.8	37	32				
1500	1.5	25	24				
2000	2.4	31	28				
3000	2.8	29	27				
4000	3.5	30	28				

**B 71**

Unaltered			
<i>Frequency</i> [Hz]	<i>Input</i> <i>Voltage</i> [V <sub>rms</sub> ]	<i>T<sub>c</sub></i>	<i>T<sub>f</sub></i>
0	1	35	31
100	1	35	32
200	0.8	29	28
300	0.8	28	27
400	0.8	27	26
500	0.5	22	22
800	0.8	24	24
900	0.8	24	24
1000	1.8	31	30
1500	1.8	28	28
2000	3	33	33
2500	3	31	31
4000	3	29	29

## Appendix B

The transfer function for the temperature model described in section 4.1.4.

$$H_1(s) = \frac{\theta_{fa}}{s^2 \theta_{cf} \theta_{fa} C_1 C_2 + s(\theta_{cf} C_1 + \theta_{fa} C_1 + \theta_{fa} C_2) + 1}$$

$$H_2(s) = \frac{\theta_{cf} + s\theta_{cf} \theta_{fa} C_2 + \theta_{fa}}{s^2 \theta_{cf} \theta_{fa} C_1 C_2 + s(\theta_{cf} C_1 + \theta_{fa} C_1 + \theta_{fa} C_2) + 1}$$

$$a = \frac{1}{\theta_{cf} \theta_{fa} C_1 C_2} \quad b = \frac{\theta_{cf} C_1 + \theta_{cf} C_2 + \theta_{fa} C_2}{\theta_{cf} \theta_{fa} C_1 C_2}$$

$$T_f(s) = \frac{P}{s} \theta_{fa} a \frac{1}{s^2 + sb + a} = \frac{P}{s} \theta_{fa} a \frac{1}{(s + p_1)(s + p_2)}$$

$$\begin{aligned} T_c(s) &= \frac{P}{s} \left( (\theta_{cf} + \theta_{fa}) a \frac{1}{s^2 + sb + a} + \frac{1}{C_1} \frac{s}{s^2 + sb + a} \right) = \\ &= \frac{P}{s} \left( (\theta_{cf} + \theta_{fa}) a \frac{1}{(s + p_1)(s + p_2)} + \frac{1}{C_1} \frac{s}{(s + p_1)(s + p_2)} \right) \end{aligned}$$

$$p_{1,2} = \frac{b}{2} \pm \sqrt{\left(\frac{b}{2}\right)^2 - a}$$

$$T_f(t) = P \theta_{fa} a \frac{p_2 e^{-p_1 t} - p_1 e^{-p_2 t} - p_2 + p_1}{p_1 p_2 (p_1 - p_2)} + T_a$$

$$T_c(t) = P \left( (\theta_{cf} + \theta_{fa}) a \frac{e^{-p_2 t} - e^{-p_1 t}}{p_1 - p_2} + \frac{1}{C_1} \frac{p_1 e^{-p_1 t} + p_2 e^{-p_2 t}}{p_1 - p_2} \right) + T_a$$